1 **Seasonal Sinking rates of Transparent Exopolymer Particles (TEP) concentrations with**

2 **associated Carbon flux in adjacent Bohai Sea and Yellow Sea**

3 M Shahanul Islam[1,2,3], Sun Jun[2,3*], Li Xiaoqian[2,3], Leng Xiaoyun[2,3]

4 1. College of Food Engineering and Biotechnology, Tianjin University of Science and

5 Technology University, Tianjin 300457, China

6 2. Tianjin Key Laboratory of Marine Resources and Chemistry, Tianjin University of

7 Science and Technology, Tianjin 300457, PR China

8 3. Research Centre for Indian Ocean Ecosystem, Tianjin University of Science and

9 Technology, Tianjin 300457, China

10 *Corresponding Author: phytoplankton@163.com

11 **Abstract**

12 Experiments on seasonal distributions and sedimentation of transparent exopolymer

13 particles (TEP) and its impacts on carbon cycle were done at three different depths in the

14 Bohai Sea (BS), North Yellow Sea (NYS) and South Yellow Sea (SYS). Total 56 stations

15 were sampled for TEP and its sinking rate by SETCOL method during autumn (2014),

16 summer (2015) and winter (2015). Temperature, phytoplankton, chlorophyll-a (Chl-a) and

17 salinity with five nutrients, phosphate (DIP), silicate (DSi), dissolved inorganic nitrate (DIN)

18 (including nitrite, nitrate and ammonium) samples were also collected and measured for

19 correlation analysis to visualize the seasonal effects on TEP concentrations and its sinking.

20 Average of total TEP (2.13 μg Xeq L^{-1}) was higher in NYS (3.32 μg Xeq L^{-1}) costal currents

21 with highest average TEP during winter (6.17 μg Xeq L^{-1}) specially in NYS (7.00 μg Xeq L^{-1})

22 through coastal current mixing zone. Average of total sinking rates (1.03 mD^{-1}) was higher

23 in SYS (1.09 mD^{-1}) through mid-water layer than other seas, especially in autumn (1.13 mD^{-1})

24 with higher seasonal average sinking rates at summer (1.04 mD^{-1}). Carbon associated with

25 TEP (TEP-C) was averagely distributed (1.47 μg C L^{-1}) at subsurface layer of study areas.

26 Seasonal highest distribution of TEP-C was 4.44 μg C L^{-1} during winter, mostly in NYS.

27 Dominant phytoplankton species *Paralia sulcata, Thalassisira excentrica* and *Rhizosolenia*

28 *styliformis* maintained average correspondences with TEP which may indicate the influences

29 of them on TEP concentration. Coastal stations were averagely clustered together in

30 multivariate analysis after congregating oceanic stations in other groups. Species based

31 relations were generated by Pearson correlation analysis. CCA revealed that average close

32 correspondence of TEP with Chl-*a* during autumn and with nutrient during winter.

1 Introduction

Transparent exopolymer particles (TEP) are macro-gels like substances that play an active role between the particulate and dissolved organic carbon pools (POC and DOC, accordingly), by extending the size continuum, in addition to assisting particle formation in the marine carbon cycle (Alldredge et al., 1993; Passow, 2002b; Verdugo et al., 2004). TEP are generally considered as transparent particles which can be stainable by Alcian Blue, a dye that favorably binds to acidic polysaccharides after complexing with carboxyl groups and sulfate (Alldredge et al., 1993; Passow and Alldredge, 1995). Abiotically TEP produced from dissolved polysaccharide secretion by phytoplankton (Logan et al., 1995; Passow, 2002b; Thuy et al., 2015). As TEP possess surface-active characteristics with neutral buoyancy, they are scavenged easily with gas bubbles (Wurl et al., 2011a; Wurl and Holmes, 2008) and aggregated at the sea surface layer which can make organic sea surface microlayer (SML) accordingly (Azetsu-Scott and Passow, 2004; Cunliffe et al., 2013; Mopper et al., 1995; Wurl et al., 2009) to contribute in the increment of sea spray aerosols produced from film droplets (Aller et al., 2005).

A combined effect of regional biological and physical factors, including salinity, air-driven turbulence and production of dissolved polysaccharide primer by phytoplankton and bacteria can control the formation and distribution of TEP. Fluctuations of Nutrients availability can control phytoplankton community which is one of the relative factors that thrust the partitioning of organic matter between particulate and dissolved phases (Carlson et al., 1998; Conan et al., 2007; Lomas and Bates, 2004; Thornton, 2014). It also influences the source of organic matter and production of TEP (Claquin et al., 2008; Corzo et al., 2000; Mari et al., 2005; Passow, 2002a). Relationships between TEP and chlorophyll *a* (Chl-a) develop during a bloom, resembles the production of TEP by phytoplankton (Passow, 2002b). This relationship during bloom phase is species-specific, with the cellular aggregation rate of TEP by phytoplankton caused by their growth period. So, relation patterns of TEP and chl-*a* will not match due to the variations in phytoplankton compositions with different life stages. Low nutrient increases TEP abundances through preventing TEP consumption by bacteria (Bar-Zeev and Rahav, 2015), so that aggregation and accumulation

64 of TEP at the sea surface as N-poor C-rich organic material (Passow, 2002b, Mari et al.,
65 2017).

66   TEP are more adherer than non-TEP substances which may help in particles and
67 subsequently increase sedimentation (Logan et al., 1995; Passow et al., 1994). As microbial
68 hotspots, TEP and POC serve a source of carbon to the deep ocean by sinking in the water
69 column (Jokulsdottir and Archer, 2016; Prairie et al., 2015). Although sinking process of
70 marine aggregates have been observed (Burd and Jackson, 2009; Iversen and Robert, 2015),
71 there remains the necessity of understanding about the effect of TEP in the biological carbon
72 pump (Burd et al., 2016; Zetsche and Ploug, 2015). TEP sinking rate measurement
73 experiments in Changjinag (Yangtze River) estuary near East China Sea during summer
74 showed higher sedimentation of TEP at the upper water column than deep seas (Guo & Sun
75 2018). It also showed the higher sinking rat of TEP in the summer rather than spring which
76 may have important role on carbon exports in that area.

77   The present study was conducted through the semi-closed Bohai Sea (BS) and Yellow
78 Sea which covered a big part of the north Chinese seas. Semi enclosed BS is located at the
79 north-eastern continental region of China (Xu et al. 2010). With sensitive primary
80 productivity and commercial fishery (Tang et al. 2003, Huang et al. 1999), BS got waste
81 water-loads and inputs from the Tianjin City as well as Liaoning, Shandong and Hebei
82 provinces (Xu et al. 2010). There is another semi-enclosed marginal sea of the western
83 Pacific Ocean at the southern-east of BS, called Yellow Sea (Liu et al. 2015b). Yellow Sea
84 possesses various oceanic processes through seasons (Hwang et al. 2014; Su 1998; Yuan et
85 al. 2008; Isobe 2008). Zonation of Yellow Sea i.e. North Yellow Sea (NYS) and South
86 Yellow Sea (SYS); will help in visualization of better seasonal scenario (Li et al. 2017). In
87 autumn, appurtenance of Yellow Sea cold water mass (YSCW) at SYS influenced the vertical
88 mixing of NYS water (Zou et al. 1999). The Yellow Sea Warm Current (YSWC) acted at
89 SYS during winter (Gao et al., 2004, Su 1998) and Changjiang Diluted water (CDW) during
90 summer (Naimie et al. 2001). Fishery (Tang and Su, 2001), biological community (Hyun and
91 Kim, 2003; Fu et al., 2009; Zhang et al., 2009) and ecological problems raises the importance
92 of researches on Yellow Sea (Sun et al., 2011; Tang et al., 2007, 2010).

93   Studies on TEP and its sinking rates showed correlation with environmental
94 parameters i.e. temperature (Claquin et al. 2008, Fukao et al. 2012), salinity (Mari et al.
95 2012), microbial breakdown (Mari et al. 2017) and phytoplankton species composition

(Passow 2002b). Changes in TEP assemblage may also influenced by bacterial secretions and feeding as well as zooplankton grazing locally (Passow and Alldredge, 1999, Surosz et al. 2006, Mari et al. 2017). It also showed correlation with nutrients in different studies (Corzo et al. 2000, Mari et al 2005). Seasonal variation of parameters can be a cause behind these phenomena. Poor correlations among TEP and these environmental parameters can be found due to limited data and insignificant variations in salinity and nutrients from sampling stations (Guo & Sun 2018). Seasonal distribution and sinking rate of TEP will describe more specific relation of TEP with other environmental parameters. On the basis of these objectives, present study was conducted on sinking flux of TEP and its concentration with related carbon exports through three separate seasons (autumn, summer, winter) in the Bohai and Yellow Sea of China from 2014-2015.

2 Materials and Methods

2.1 Study area and sample collection

Water sample (1 liter) was taken from three different depths (0-100 meters) at various stations (Fig. 1) during 2014-2015 in Bohai Sea (BS), North Yellow Sea (NYS) and South Yellow Sea (SYS). Session for autumn sampling was conducted between 8-22 November (Fig. 1A), 2014, summer sampling from 18 August to 22 September, 2015 (Fig. 1B) and winter sampling in Bohai Sea and North Yellow Sea from 17 October to 22 November, 2015 (Fig. 1C). Boundary currents flow directions in Bohai Sea and Yellow Sea were changed with seasons (Fig. 2). Korean coastal currents (KCC) flows northward in summer and southward in winter. YSWC was found during winter and CDW flows eastward during summer. Remain costal currents and warm currents flows in their constant direction (Hwang et al. 2014; Su 1998; Yuan et al. 2008; Isobe 2008) which may have distributary effect on these particles concentration and its sinking rates besides all hydrological parameters.

Sample collection was done by multiple rosette (with CTD sensors) for different depths at each sampler stations based on bottom depth. Each station wat designed with three distinguishing depths for better graphical analysis. Samples were collected seperately to determine phytoplankton composition, chl-*a* concentration, nutrients, TEP abundances and its sinking rates. Due to shallow water, depths were limited in each station between 0-100 meters. In 1L sampling bottles, phytoplankton samples were collected with 1% formaldehyde concentration for further analysis (Guo and Sun 2018). Sea water were collected in 100 mL sample bottle from all sampling depths and stored at -25°C for nutrient analysis of each

station. CTD sensors recorded temperature and salinity was determined while sampling from different depths from study area.

2.2 Biological parameters

According to Welschmeyer (1994), chlorophyll – a (chl a) were measured after filtering seawaters from all stations by 25 mm GF/F filters (Whatman^{TM}) and then reserved at -20°C in the dark until analysis. 90% acetone were used for extraction of chl-a for 24 h at -20°C in the dark, and samples were then analyzed by a laboratory fluorometer called Turner-Designs Trilogy^{TM}. Phytoplankton sample (1 Liter, preserved with 1% formaldehyde) were analyzed according to modified Utermöhl methods followed by Sun et al. (2002) after arranging the samples (25 mL) in Utermöhl counting chamber (being settled for 24 hrs.) in inverted microscope. Dominance index was used to describe phytoplankton dominant species under this equation:

$$Y = \frac{n_i}{N} \times f_i$$

Where, N is the total cell abundance of all species, n_i is total cell of species i and f_i is the count of occurrence of species i in all sample (Guo et al. 2014).

2.3 Chemical analysis

Nutrients i.e. dissolved inorganic phosphate (DIP), dissolved inorganic nitrogen (DIN), dissolved silicates (DSi), ammonium, nitrate & nitrite analysis were measured by fully automated (SANPLUS, Dutch SKALAR company) wet chemical analyzer (Liu et al., 2015a). Sextuplicate measurements of TEP were done by following colorimetric method of Passow and Alldredge (1995) for all samples after confirming calibration factor (f_x) from xanthan gum curve. At least 50 mL (V_f) sample sea water were thoroughly filtered (4-6 replicates) at low and fixed vacuum (150 mm of Hg) through polycarbonate filters (0.4-pm pore-size) and dye binding particles on the filter for approximate 2 seconds with 500 micro liters of 0.02% alcian blue (8GX; aqueous solution) in 0.06% acetic acid (pH 2.5). After staining, filters are rinsed carefully with distilled water to prevent excess dye once. Dye bound to substrates will not wash off by this rinsing. Then filters were soaked into 25 mL beakers with 6 mL of 80% sulfuric acid and kept for 2 hours. The beakers were gently shacked for 3-5 times during soaking period. Maximum absorption of the solution (E_{787}) lied at 787 nm and it was measured (μg Xeq. L^{-1}) in a l cm cuvette (B_{787}) against distilled water as a reference. The equation is:

$$TEP = (E_{787}-B_{787}) \times (V_f)^{-1} \times fx$$

Where, fx = Average calibration factor and it was 9.83 µg from the graph of xanthan gum curve. Calculation of TEP-carbon (TEP-C, µg C L^{-1}) was determined with the slope (0.75) from the equation as follows (Engel &Passow 2001):

$$TEP\text{-}C = 0.75 \times TEP_{color} \text{ (Guo \& Sun 2018)}$$

where TEP$_{color}$ is the TEP concentration (TEP) with the unit of µg Xeq L^{-1}.

2.4 Measurement of TEP sinking flux

TEP sinking rates were determined at each station, and the SETCOL method was used to measure the sinking rates on research vessel according to Bienfang (1981). For measurements, a Plexiglass column (height = 0.45 m and volume = 750 mL) was filled completely with a homogeneous water sample within 10 min after sampling, and a cover was then placed on the set-up. The Plexiglass columns were kept undisturbed on the vessel to settle for 2-3 hours. Temperature was maintained through a thermostatically controlled water bath with water jackets by pumping its water. The settled sample of experiment was collected in sample bottles by successively draining the upper, middle, and bottom compartments of the Plexiglass column via piped outlet in the wall of column. The TEP biomass was measured after the settlement in the samples from all three compartments. These measurements were combined to calculate the sinking rate of TEPs according to the formula:

$$TEP_s = \frac{B_s}{B_t} \times \frac{L}{t}$$

where V = sinking rate; B$_s$ = the biomass of TEP settled into the bottom compartment; B$_t$ = the total biomass of TEPs in the column; L = length of the column; and t = settling interval. Samples from all depts were triplicated during measurement for better data analysis and marked according to stations about sinking rate as well as TEP concentrations.

2.5 Data analysis

Analysis and discussions were forwarded with seasonal (autumn, summer & winter) and oceanic (Bohai Sea, North Yellow Sea & South Yellow Sea) categories accordingly (Table 1). Various multivariate analyses were performed by using Multi Biplots software (Vicente Villardón, 2015) on recorded data. Single cluster analysis was performed by Multivariate Statistical Package Software with Baroni-UrbaniBuser Coefficient. Linear regression,

188 Pearson correlation and covariance were performed by Microsoft Excel 2016 software.
189 Canonical correspondence analysis (CCA) were done by Canoco software, version 4.14
190 (CANOCO for Windows; Ter Braak & Šmilauer, 2002). For integrated surface view of
191 recorded and examined parameters during winter 2015, Surfer 12 was used. Box-whisker
192 plots by Microsoft Excel 2016 showed the range of recorded TEP and TEP$_s$ through different
193 water layers after stations' integration. Concentrations of different parameters were
194 graphically presented by Ocean Data View (ODV 2016) software.

3 Results

3.1 Environmental Hydrology

197 Study stations were segmented on the basis of sea for better understanding about
198 present observtions during autumn 2014 (Fig. 1A), summer 2015 (Fig. 1b) and winter 2015
199 (Fig. 1C). Sampling stations (St.s) of autumn through the Bohai Sea (St.s B45 - B68), North
200 Yellow Sea (St.s B04 - B34) and South Yellow Sea (St.s H07 - H40) were determined by
201 geographical positions (Fig. 1D). Similarly, the stations of Bohai Sea (St.s B45 - B68), North
202 Yellow Sea (St.s B04 - B34) and South Yellow Sea (St.s H07 - H38) were associated
203 accordingly in summer. In winter, sampling was done only in Bohai Sea (St.s B42 - B68, BS1
204 & BS5) and North Yellow Sea (St.s B04 - B33), except SYS.

205 The Bohai Sea and Yellow Sea had a complex dynamic environment with various
206 seasonal and local geophysical currents (**Fig**. 2). Seasonal currents flow maps (Fig. 2) were
207 drawn on the basis of secondary data and previous literatures (Hwang et al. 2014; Su 1998;
208 Yuan et al. 2008; Isobe 2008) from that area due to track the possible water mass effect on
209 TEP distribution. Average concentration of all parameters through every season showed high
210 chl-*a* concentration along coastal zones of BS and NYS. Average annual TEP was higher at
211 BS along BSCC, at NYS along YSCC and at SYS along CDW. Average annual nutrients
212 were highly concentrated at BS than other seas, except nitrite at YSCC of SYS (Table 1).
213 Adequate T-S diagrams noted out stations aggregations at different seasonal water masses
214 through seas i.e. low temperature low salinity (LTLS), low temperature high salinity (LTHS),
215 high temperature low salinity (HTLS) and high temperature high salinity (HTHS)
216 accordingly (Fig. 3). All stations of BS were scattered at LTLS (Fig. 3A) and NYS at LTHS
217 (Fig. 3B) during autumn due to lower sampling depth, influenced by surface mixing. SYS
218 were segmented into HTHS and LTHS in both autumn (Fig. 3C) and summer (Fig. 3F);
219 followed by NYS in summer only (Fig. 3E). Due to high surface temperature, stations with

3.1.1 Vertical concentrations in autumn 2014

During autumn (Fig. 4A), TEP was higher at the north of NYS along LCC and CWC of southern SYS (Fig. 4D). Temperature were higher at YSCC of SYS and salinity were dense at KCC of NYS and SYS with high Chl-a was at LCC of NYS. Concentrations of nutrients were higher at BS except nitrite. Nitrite was higher at LCC of NYS and at YSCC of SYS. DIP. DIN, DSi and nitrate were higher at the southern part of SYS through whole autumn (Table 1). Vertical profile showed higher concentration of TEP of SYS with high temperature too, especially at St. H33, H35 and H40. Chl-a was dense in NYS (St. B15, B19 and B25) where DSi was dramatically low. Nutrients i.e. DIN, nitrate and ammonium were found higher at the bottom of BS, especially at St. B45, B49 and B57. Salinity was lower at surface of whole study area. DIP found lowest at surface stations i.e. H07 and H09 of SYS but highest at bottom of B34 and H07 stations. Nitrite was found higher at the SCM of NYS and SYS (Table 1). During autumn, dominant phytoplankton were *Paralia sulcate, Coscinodiscus* sp.*, Ceratiumfusus, Thalassiosira sp., Probosica alata f. indica, Ceratiumtripos, Nitzschia* sp.*, Thalassiosira pacifica, Guinardia delicatula* and *Thalassiosira excentrica* sequentially.

3.1.2 Vertical concentrations in summer 2015

Through summer (Fig. 4B), TEP was higher at southern SYS (Fig. 4E) with high temperature and nutrients (DIP, DIN, DSi and nitrates). Notably, DIP found high at CWD of SYS. In BS, nitrate and nitrite were higher at south coast and ammonium was higher at north-west coast with high temperature. Salinity was aggregated at KCC of NYS and mid SYS. Chl-a was dense at YSCC of NYS and CDW of SYS (Table 1). With obvious high temperature, summer possessed low TEP at surface of BS. TEP was higher with low nutrients and chl-a at the SCM of Station B45. DIN, nitrate and nitrite were high near station B68. DIP and DSi were higher at the bottom of Station B57 in BS. TEP was comparatively low at NYS with high chl-a at SCM and bottom of Station B25. DIP, DSi and nitrate were higher at the bottom of Stations B04 and B11. *Alexandrium tamarense, Rhizosolenia styliformis, Paralia sulcate, Guinardia flaccida, Dinophysis sp., Ceratium fusus, Thalassiosira excentrica, Ceratium furca, Dictyocha fibula* and *Diploneis bombus* were dominant phytoplankton accordingly through study area in summer. In SYS, TEP was higher at the SCM with low

8

nutrients and chl-a as BS (Fig. 4E). Nutrients along with salinity were higher at the bottom of Station H-7 and H09.

3.1.3 Vertical concentrations in winter 2015

In winter (Fig. 4C), TEP was dense at KCC of NYS, especially at SCM (Fig. 4F) with high temperature and salinity. However, chl-*a* was higher at the north coast and BSCC of BS with YSCC of NYS too. Most of the nutrients were higher at BSCC of BS except DIP. DIP found higher at the transitional zone of BS and NYS.DSi concentration was also higher at KCC of NYS. During winter, NYS showed higher abundances of Chl-a and salinity at the stations (B04, B25 & BS5) near YSCC. Higher TEP was found at SCM of NYS than BS. Temperature was recorded lowest in BS than NYS (**Fig**. 1), especially near shore area. Phytoplankton i.e. *Paralia sulcate*, *Thalassiosira excentrica*, *Actinoptychus* sp.*, Donkinia recta*, *Thalassiosira sp.*, *Coscinodiscus* sp., *Coscinodiscus subtilis*, *Navicula* sp.*, Pleurosigma pelagicum* and *Coscinodiscus radiatus* were dominant during winter. Nutrients i.e., DIN, DSi, ammonium, nitrate and nitrite found higher at the SCM of Bohai Sea. DIP was found abundance in surface area at the transitional area (near Station B33) of BS and NYS (Table 1). Average nutrients were higher in BS than NYS during winter 2015. Stations near coastal area of BS (B45 & B68) and NYS (B04, B25 & BS5) have higher nutrients comparatively.

3.2 Seasonal and regional TEP concentration with carbon association

Present study measured 2.13 μg Xeq. L^{-1} as average TEP concentration (TEP) which is ranged between 0.2-23.20 μg Xeq. L^{-1}. NYS (2.32 μg Xeq. L^{-1}) has more TEP concentration in average than SYS (1.18 μg Xeq. L^{-1}) and BS (2.08 μg Xeq. L^{-1}). Apparently, winter season (6.17 μg Xeq. L^{-1}) shows higher average concentration of TEP in each sea (Table 1) than in summer (1.10 μg Xeq. L^{-1}) and in autumn (0.67 μg Xeq. L^{-1}). SYS showed higher TEP in autumn (0.93 μg Xeq. L^{-1}) and in summer (1.42 μg Xeq. L^{-1}) at HTHS (Fig. 5C & 5F). In BS, assemblage of TEP was higher at LTLS during summer (Fig. 5D) than autumn (Fig. 5A). Apparently, TEP was higher at LTHS of NYS during summer (Fig. 5E) and winter (Fig. 5G) than autumn (Fig. 5B).

The carbon (TEP-C) associated with TEP picked at winter 2015 and became lower during autumn 2014. BS showed low carbon abundance at surface during summer (Fig. 6E). NYS possessed high TEP-C in SCM during winter (Fig. 6J) and at bottom during autumn and summer (Fig. 6B & 6F). Surface of SYS recorded high TEP-C than BS and NYS during summer (Fig. 6G). However, SYS also possessed comparatively high verity of TEP-C than

BS and NYS at its SCM during autumn and summer (Fig. 6D & 6H). Average TEP-C showed high variation at SCM through study areas (Fig. 6L). Average TEP-C was 1.47 µg C L^{-1} with seasonal highest 4.44 µg C L^{-1} during winter specially in NYS (5.25 µg C L^{-1}). SYS has higher TEP-C during autumn (0.58 µg C L^{-1}) and summer (1.07 µg C L^{-1}) than other seas. Highest TEP-C was found at SML of stations B15 (15.78 µg C L^{-1}), B22 (17.40 µg C L^{-1}) and B33 (10.91 µg C L^{-1}) of NYS during winter which showed close cluster during analysis (Fig. 9C; Grpup 8).

3.3 Seasonal and regional TEP sedimentation

Sedimentation or sinking rates of TEP was recorded 1.03 mD^{-1} in average of all seasons (Table 1) at study area. TEP sinking rate was higher in summer (1.04 mD^{-1}) than autumn (1.02 mD^{-1}) and winter (1.03 mD^{-1}). However, winter showed high sinking rates (1.02 mD^{-1}) in BS than its summer (1.01 mD^{-1}) and autumn (0.9 mD^{-1}) data. On the other hand, comparatively high sinking rates were measured in SYS during autumn (1.13 mD^{-1}) than its summer (1.05 mD^{-1}). SYS also possessed average high sinking rates of TEP (1.09 mD^{-1}) than BS (0.9 mD^{-1}) and NYS (1.03 mD^{-1}).

3.4 TEP sinking in segmented depths

Average TEP sinking dynamics were similarly close in average at each depth (Fig. 7K). In BS, high sedimentation variation was observed at mid layer (Fig. 7A) during autumn (0.72-1.16 mD^{-1}) and at surface (Fig. 7E, 7I) during summer (0.86-1.57 mD^{-1}) and winter (0.64-2.06 mD^{-1}). Surface of NYS (Fig. 7B) has diverse sinking rates during summer (0.77-2.47 mD^{-1}), mid layer (Fig. 7F) in winter (0.72-1.53 mD^{-1}) and bottom (Fig. 7J) in autumn (0.76-1.19 mD^{-1}). Surface of SYS (Fig. 7C) during summer (0.62-2.40 mD^{-1}) and bottom layers (Fig. 7G) during autumn (0.78-1.55 mD^{-1}) showed sedimentation variation accordingly. In average, bottom layer (Fig. 7D) during autumn (0.72-1.55 mD^{-1}) and surface of study area during summer (0.62-2.47 mD^{-1}) and winter (0.64-2.06 mD^{-1}) possessed high sinking dynamicity (Fig. 7D, 7H & 7L).

3.5 Correspondence relationships of TEP

TEP showed close correspondent relationship with DIP and chl-*a* in average (Fig. 8I) and in winter at BS (Fig. 8F) after applying CCA. However, winter at NYS showed TEP was corelated with nitrate through each station. In autumn, TEP showed average close correspondence with nitrite in CCA across study areas (Fig. 8A, 8D, 8G & 8J). During

summer, TEP was averagely compliance with nitrite (Fig. 8D) through all seas (Fig. 8H and 8I) except at BS (nitrate; Fig. 8E). In average, TEP showed close correspondences with *T. excentrica* and *P. sulcata* during autumn, *R. styliformis* in summer and *P. sulcate* and *Actinoptychus* sp. were dominant across study area. Both in BS and NYS, *P. sulcata* was highly dominant and mostly correlates with concentration of TEP through all seasons. In SYS, correspondences of dominant phytoplankton with TEP were observed rather than nutrients (Fig. 8J & 8K).

Considering all parameters, most of the SYS stations clustered closely in dendrogram (Group 1 and 4) after applying Baroni-Urbani Buser coefficient during autumn (Fig. 9A) and summer (Fig. 9B). In BS, St. B45 clustered in same group with B68 through all season (autumn; group 2, summer; Group 5 and winter; Group 7). St. B15 of NYS showed group correspondence with St. B25 during autumn (Fig. 9A; Group 2) and winter (Fig. 9C; Group 8) except summer. Rest of the stations clustered randomly with each other due to their different gradients.

4 Discussions

4.1 Seasonal effect on TEP distribution

Study of seasonal trends on EPS (exopolymeric substances i.e. TEP) confirmed the formation of EPS at earlier season in upper sea column with time (Riedel et al. 2006, Collins et al. 2008). Traditionally, phytoplankton cells were reported as precursors of TEP, especially under bloom situations (Hong et al. 1997; Passow 2002a; Passow and Alldredge 1994). Moreover, Changes in TEP influenced by a balance between sources i.e. production by algae, bacteria, and possibly other organisms (Ortega-Retuerta et al. 2010). In BS, *Skeletonema costatum* and *Coscinodiscus oculus-iridis* during winter and *Noctiluca scintillans, Chaetoceros affinis, Chaetoceros* sp. through all seasons were reported as dominant phytoplankton species (Yang et al. 2018) which may have local influence on TEP (Passow 2002a). However, *P. sulcata* showed dominancy in BS through 3 seasons BS by corresponding closely with TEP (Fig. 8D, 8E & 8F). During autumn at NYS, *Pseudo-nitzschia pungens* and *Proboscia alata* were reported dominant at the same location of dense TEP compared to present study (Li et al. 2017) which may also liable for TEP assemblages by demonstration close relation in CCA (Fig. 8G). In SYS, dominancy of *Paralia sulcate* and *Thalassiosira angulate* (Li et al. 2017, Liu et al. 2015a) with *Pseudo-nitzschia pungen* (Li et al. 2017) were reported at same magnitudes during autumn which were similar to present

study and also maintained close correspondences with TEP (Fig. 8J). Coastal SYS showed the dominancy of *Skeletonema costatum* and *Thalassiosira nordenskiodii* during winter (Wen et al. 2007). Among phytoplankton, cyanobacteria (36%) were reported stratified during summer at SYS (Liu et al. 2015b). Phytoplankton i.e. *Paralia sulcata*, *Prorocentrum dentatum* and *Thalassiosira angulata* were abundant species at south of SYS which area were highly concentrated with TEP (**Fig. 6**A) according to present study. Biological process of these species may liable for the abundance of TEP along with those study areas.

However, TEP can be high in lower biological activity (Mari et al. 207). In absence of phytoplankton, dissolve organic matter can be source of TEP (Wurl et al. 2011b). During autumn and summer, TEP was abundant with high nutrients and low Chl-*a*. Arctic autumn showed low TEP concentrations in upper water layer with no significant enrichment (Wurl et al. 2011). Though, limited sampling data showed no significant correlation of TEP with nutrients and salinity in Changjinag (Yangtze River) estuary (CE) near East China Sea (Guo & Sun 2018). However, TEP was higher along CDW from CE during this study at summer. Consumption by various organisms (Tranvik et al. 1993) can also change TEP distribution. In some places, organisms may feed on TEPs due to low nutrient concentration which is why TEP is very low in those areas during summer and autumn (**Fig**. 4). Higher tempered zone also possessed high TEP production due to the effect of temperature on photosynthetic parameters (Claquin et al. 2008, Fukao et al. 2012) which supported high TEP assemblage at HTLS through BS during summer (Fig. 5D) and at HTHS of SYS during summer and Autumn (Fig. 5C & 5F). It also influenced high TEP concentrations in various estuaries and seas during summer and spring than other seasons (Table 4). Semi enclosed Aegean Sea was reported with increased TEP during summer than autumn due to phytoplankton production and bacterial activity (Parinos et al. 2017). Similar seasonal TEP pattern was observed at semi embedded BS (Table 1) which also possessed close correspondences with dominant *P. sulcate* (Fig. 8E)*.

During summer, TEP was high at CDW generating Changjinag (Yangtze River) estuary near East China Sea than spring due to high primary productivity (Table 4; Guo & Sun 2018). Similarly, TEP was also found higher near CDW cruising area of SYS during summer (Fig. 4B) with high chl-*a* than others seas (Table 1). Arctic winter season also showed the highest TEP concentrations and formation rates until spring due to algal activity (Wurl et al. 2011b) which interprets prior TEP concentration during winter than other seasons with high chl-*a* along study areas (Table 1). Species' closer correspondences with TEP during

winter (Fig. 8C) and summer of SYS (Fig. 8K) also supported these statements. Notably, Oligotrophic reservoir was also reported with high TEP during summer than other seasons (Vicente et al. 2009).

Studies showed that mostly estuaries possessed higher average TEP at 0-50 m than bays and open seas due to higher primary productivity (Table 2). However, literatures demonstrated that highest TEP was found at the surface water column in Adriatic Sea (Radic et al. 2005) and lowest in Weddell Sea (Ortega-Retuerta et al. 2009). Average TEP was higher in western subarctic part (Ramaiah et al. 2005) than eastern (Wurl et al. 2011b) and western tropical parts (Kodama et al. 2014) as well as eastern subarctic zone (Wurl et al. 2011b) at ocean (Table 2). Higher estuarine TEP was found in Changjinag River Estuary (Guo & Sun 2018) during both in summer and spring rather than that of Jiulong River estuary (Peng and Huang 2007) and Pearl River estuary (Sun et al. 2010). Upper water column observed lower average TEP at LTLS of BS than in Chesapeake Bay (Malpezzi et al. 2013) and Gulf of Cadiz (Garc et al. 2002). However, surface water column of North Pacific Ocean possessed higher TEP than below 50 meters due to high biological production (Table 3). Consequently, average seasonal TEP concentration was found higher at surface water column of study area (Fig. 4).

Similarly, deep water column of bays was reported with high TEP concentration than seas and open oceans due to higher primary production (Table 3). Gulf of Aqaba showed highest TEP below 50 meters of any seas (Bar-Zeev et al. 2009). Deep water column of Aegean sea was reported with high TEP during autumn (Parinos et al. 2017) which is similar to SYS (St.s H35 & H40; Fig. 4D) through same season. Below 100m, TEP was higher in Eastern Mediterranean Sea (Bar-Zeev et al. 2011) than other part of this sea (Ortega-Retuerta et al. 2010) and Gulf of Aqaba (Bar-Zeev et al. 2009). Average vertical TEP profiling was higher in Ross Sea (Hong et al. 1997) than rest seas (Table 2). Bacterial activity and phytoplankton excretions were liable for these dispersion (Parinos et al. 2017, Mari et al. 2017). Average TEP was observed high at LTHS (Fig. 3G) in Bohai Sea (Fig. 5C) through BSCC (Fig. 2C) during winter (Fig. 4C) with highest chl-*a* (Table 1). High productivity may initiate these phenomenon (Wetz et al. 2009). However, LTHS of NYS showed high TEP during winter (Fig. 5G) than other seasons (Fig. 5B & 5F). On the other hand, SYS picked high TEP at HTHS during autumn (Fig. 5C) than rest seasons (Fig. 5F). Combined effects of seasonal environmental parameters may cause these variations through those water columns.

4.2 Seasonal sinking rate variations of TEP

Sinking rates or particle sedimentation of TEP can also cause changes in TEP distribution (Passow et al. 2001). SETCOL method was most popular scientific method to track it due to its simplicity and reliability (Guo & Sun 2018). However, motion and turbulence of seawater was ignored in SETCOL which have complex effect on particle sinking in ocean (Javier et al. 1996, Ruiz et al. 2004). So, the actual situation remained unclear with theories (Guo & Sun 2018). Seawater is denser than TEP (density 0.70-0.84 g cm^{-3}) which indicated that pure TEP will ascend upward in ballast free condition (Azetsu-Scott and Passow 2004). So, sinking rates of TEP can be negative (Azetsu-Scott and Passow 2004, Mari 2008). In real scenario, presence of organic and inorganic matter in seawater make complex situation for TEP to be pure. Sticky gel characteristics of TEP (Engel 2000, Rochelle-Newall et al. 2010) may aggregated them with various detritus, particles and organisms i.e. bacteria, phytoplankton and mineral clays (Prieto et al. 2002) which may influence them to sink downward in water (Mari et al. 2017).

Freshwater lake has lower particle concentration with higher sinking rates of TEP (Table 7) due to the influence of phytoplankton cells aggregation (Vicente et al. 2009). Estuarine TEP sedimentation rate was reported lower in spring than other seasons (Guo & Sun 2018). Through seas, Average sinking rate of TEP in NYS (Table 5) was observed higher in summer and winter during present study may be due to higher salinity (Table 1) and primary productivity (Chl-a). Oligotrophic reservoir was also reported with high sinking rates during late winter and early spring (Vicente et al. 2009). In SYS, highest TEP sedimentation was at Station H38 (2.40 mD^{-1}) may be caused by counter effect of CDW and CWC (Fig. 2). SYS also has higher sinking rates of TEP in autumn than BS and NYS may be due to high nutrient concentrations (Fig. 6) at the bottom that may stick with TEP to sink downwards. Rather than other coastal water (Changjiang Estuary), Bohai Sea possessed higher sinking rates of TEP in average, especially during summer (Table 5). However, open ocean was observed with low sinking rate due to is unproductive winter stratification (Mari et al. 2008). Seasonal effect on concentrations of environmental parameters and coastal currents' activity may cause these differences in sedimentation rates of TEP in study areas.

4.3 Potential role of seasonal carbon export associated with TEP

Organic carbon formations at sea surface through TEP aggregations and its sedimentation, were a complex part of the carbon cycle in ocean besides the influences of

14

besides phytoplankton cells and zooplankton fecal pellets (Turner 2002, Turner 2015, Mari et al. 2017). These exopolymer particles contained carbon complex which may disappeared due to TEP sedimentation and degradation by bacteria (Prieto et al. 2006) in the euphotic zone. Due to alignment of TEP as same magnitude of phytoplankton cells abundance (Passow 2002b, Passow et al. 2001), TEP sinking was accepted as important carbon pathway for its dominant effect on TEP-C (Stoderegger and Herndl 1999, Obernosterer and Herndl 1995, Guo & Sun 2018). Understanding TEP-C formations and its contributions along study areas, a conceptual model of TEP was drawn on the basis of TEP assemblage and its correlations with phytoplankton concentration (Fig. 10). Bacterial production and algal activity influenced the TEP assemblage at upper water column, was shown in this 3D model (Ortega-Retuerta et al. 2010, Bar-Zeev et al. 2011). Influential arrows were drawn on these literatures. CDW influences phytoplankton dominance with high concentrations at nearby ecological provinces (Li et al. 2017, Guo et al. 2014) which may influence TEP formations at southern part of SYS. TEP-C was lower in spring than in summer at Changjiang River (Yangtze River) estuary near East China Sea.

Present study observed higher total average of TEP-C in NYS than BS and SYS especially in winter and lowest TEP-C in autumn in BS during all three seasons. Lower sinking rate can increase TEP aggregation at surface area (Stoderegger and Herndl 1999, Obernosterer and Herndl 1995, Guo & sun 2018) which may influence TEP-C at NYS. Considering the complex effect of all environmental parameters, TEP-C distribution showed similar correlations with nutrients and Chl-a as TEP in different seasons accordingly. Results of present study suggest the importance of TEP in carbon cycle in Bohai Sea and Yellow Sea. TEP controlled the biological carbon pump of atmospheric CO_2 (Mari et al. 2017). With significant seasonal TEP-C distribution and TEP correlations with phytoplankton, the data showed an unavoidable importance of TEP and its sedimentation rates for exporting carbon in study areas. Stickiness of TEP and its balances between production and degradation rates contributed in POC cycling (Mari et al. 2017) in the ocean. TEP sedimentation roughly contributes 30% in POC flux at Santa Barbara Channel (Passow et al. 2001) and 0.02%-31% in oligotrophic reservoir of southern Spain (Mari et al. 2017). POC was not measured during present study. Reports showed that TEP contributes significantly in POC (Ortega-Retuerta et al. 2019). Further research may introduce from these limitations by measuring POC for stablishing significant correlations with TEP to contribute in local carbon cycle.

5 Conclusions

Seasonal variations of TEP concentration was complex and mostly depends on nutrients and Chl-a. Correlations on the basis of 168 samples of TEP with same amount of other environmental parameters showed variations among seas as well as seasons. Temperature varied from 0-28 °C round the year but TEP stacked from 0 to below 10 μg Xeq. L^{-1} in average. Biological productivity may liable for TEP distribution during autumn and summer, especially in SYS and nutrients for TEP in winter in BS. Coastal current mixing has an influence on TEP due to its dominancy at dilution zones. Sinking rates of TEP mostly varied at surface of BS and NYS during summer and winter. SYS has moderated sinking rates of TEP at its surface and bottom with higher nutrients concentrations. With close correspondences, dominant phytoplankton i.e. *P. sulcata, T. excentrica* and *R. styliformis* have influences of high TEP concentration. Average carbon exports maintained same magnitudes with TEP during each season. Average TEP sinking was diverse at SCM but higher at surface through all seasons. Further research on POC cycle by measuring TEP, TEP-C and its sinking rates with seawater density and turbidity of selected study area are recommended to be more precise on carbon contributions of exopolymers in the process of biological and chemical carbon pump in open and coastal seas.

Acknowledgements

References

Alldredge, A.L., Passow, U., and Logan, B.E.: The abundance and significance of a class of large, transparent organic particles in the ocean. Deep-Sea Res. I Oceanogr. Res. Pap. 40. http://dx.doi.org/10.1016/0967-0637(93)90129-Q, 1993.

507 Aller, J.Y., Kuznetsova, M.R., Jahns, C.J., and Kemp, P.F.:The sea surface microlayer as
508   a source of viral and bacterial enrichment in marine aerosols. J. Aerosol Sci.
509   36: 801–812. http://dx.doi.org/10.1016/j.jaerosci.2004.10.012, 2005.

510 Azetsu-Scott K. : Ascending marine particles : significance of transparent exopolymer
511   particles (TEP) in the upper ocean[J].Limnology and Oceanography，49（3
512   ）： 741-748, 2004.

513 Azetsu-Scott, K., and Passow, U. :Ascending marine particles: significance of transparent
514   exopolymer particles (TEP) in the upper ocean. Limnol. Oceanogr. 49:741–
515   748. http://dx.doi.org/10.4319/lo.2004.49.3.0741, 2004.

516 Bar-Zeev, E., and Rahav, E.: Microbial metabolism of transparent exopolymer particles
517   during the summer months along a eutrophic estuary system. Front. Microbiol.
518   6: 403. http://dx.doi.org/10.3389/fmicb.2015.00403, 2015.

519 Bar-Zeev, E.; Berman-Frank, I.; Stambler, N.; Vazqueź Domínguez, E.; Zohary, T.;
520   Capuzzo, E.; Meeder, E.; Suggett, D.; Iluz, D.; Dishon, G.; et al. Transparent
521   exopolymer particles (TEP) link phytoplankton and bacterial production in the
522   Gulf of Aqaba. Aquat. Microb. Ecol. 56, 217−225, 2009.

523 Bar-Zeev, E., Berman, T., Rahav, E., Dishon, G., Herut, B., Kress, N., and Berman-
524   Frank, I., : Transparent exopolymer particle (TEP) dynamics in the eastern
525   Mediterranean Sea. Mar Ecol Prog Ser 431: 107−118, 2011.

526 Bienfang, P.K.: SETCOL－ a technologically simple and reliable method for measuring
527   phytoplankton sinking rates. Canadian Journal of Fisheries and Aquatic
528   Sciences.38(10): 1289-1294. https://doi.org/10.1139/f81-173, 1981.

529 Burd, A., Buchan, A., Church, M.J., Landry, M.R., McDonnell, A.M.P., Passow, U.,
530   Steinberg, D.K., and Benway, H.M. : Towards a transformative understanding
531   of the ocean's biological pump: priorities for future research. Report on the
532   NSF Biology of the Biological Pump Workshop. Ocean Carbon and
533   Biogeochemistry (OCB) Program, Woods Hole, MA
534   http://dx.doi.org/10.1575/1912/8263, 2016.

535 Burd, A.B., and Jackson, G.A. :Particle aggregation. Annu. Rev. Mar. Sci. 1:65–90.
536   http:// dx.doi.org/10.1146/annurev.marine.010908.163904, 2009.

Claquin, P., Probert, I., Lefebvre, S., and Veron, B. :Effects of temperature on photosynthetic parameters and TEP production in eight species of marine microalgae. Aquat. Microb. Ecol. 51:1–11. http://dx.doi.org/10.3354/ame01187, 2008.

Corzo A, Rodriguez-Galvez, S., Lubian, L., Sangrá, P., Martínez, A., and Morillo, J.A. : Spatial distribution of transparent exopolymer particles in the Bransfield Strait, Antarctica. Journal of Plankton Research. 27(7): 635-646. https://doi.org/10.1093/plankt/fbi038, 2005.

Corzo, A., Morillo, J.A. and Rodríguez, S. : Production of transparent exopolymer particles (TEP) in cultures of Chaetoceroscalcitrans under nitrogen limitation. Aquat. Microb. Ecol. 23, 63–72, 2000.

Cunliffe, M., Engel, A., Frka, S., Gašparović, B., Guitart, C., Murrell, J.C., Salter, M., Stolle, C., Upstill-Goddard, R., and Wurl, O. : Sea surface microlayers: a unified physicochemical and biological perspective of the air-ocean interface. Prog. Oceanogr. 109: 104–116. http://dx.doi.org/10.1016/j.pocean.2012.08.004, 2013.

Engel, A, and Passow, U.: Carbon and nitrogen content of transparent exopolymer particles (TEP) in relation to their Alcian Blue adsorption. Marine Ecology Progress Series. 2001; 219: 1-10. https://doi.org/10.3354/meps219001, 2001.

Engel, A.: The role of transparent exopolymer particles (TEP) in the increase in apparent particle stickiness during the decline of a diatom bloom. Journal of Plankton Research. 22(3): 485-497. https://doi.org/10.1093/plankt/22.3.485, 2000.

Engel, A.: Direct relationship between CO2 uptake and transparent exopolymer particles production in natural phytoplankton. Journal of Plankton Research. 24(1): 49-53. https://doi.org/10.1093/plankt/24.1.49, 2002.

Engel, A.: Distribution of transparent exopolymer particles (TEP) in the northeast Atlantic Ocean and their potential significance for aggregation processes. Deep Sea Research I. 51(1): 83-92. https://doi.org/10.1016/j.dsr.2003.09.001, 2004.

566   Fu, M.Z., Wang, Z.L., Li, Y., Li, R.X., Sun, P., Wei, X.H., Lin, X.Z., and Guo, J.S.:
567   Phytoplankton biomass size structure and its regulation in the Southern
568   Yellow Sea (China): seasonal variability. Cont. Shelf Res. 29 2178–2194,
569   2009.

570   Fukao, T, Kimoto, K., and Kotani, Y.: Effect of temperature on cell growth and
571   production of transparent exopolymer particles by the diatom Coscinodiscus
572   granii isolated from marine mucilage. Journal of Applied Phycology. 24: 181-
573   186. https://doi.org/10.1007/s10811-011-9666-3, 2012.

574   Garc, C., Prieto, L., Vargas, M., et al. Hydrodynamics and the spatial distribution of
575   plankton and TEP in the Gulf of Cádiz (SW Iberian Peninsula), Journal of
576   Plankton Research, 24 : 817-833, 2002.

577   Guo, S.J., Feng, Y.Y., Wang, L., Dai, M.H., Liu, Z.L., Bai, Y., Sun, J.: Seasonal variation
578   in the phytoplankton community of a continental-shelf sea: The East China
579   Sea. Marine Ecology Progress Series. 516: 103-126.
580   https://doi.org/10.3354/meps10952, 2014.

581   Guo, S., and Sun, X.: Carbon biomass, production rates and export flux of copepods fecal
582   pellets in the Changjiang (Yangtze) River estuary. Journal of Oceanology and
583   Limnology, 36(4), 1244–1254. doi:10.1007/s00343-018-7057-1, 2018.

584   Hong Y, Smith, W.O., and White, A.M.: Studies on transparent exopolymer particles
585   (TEP) produced in the Ross Sea (Antarctica)and by Phaeocystisantarctica
586   (Prymnesiophyceae). J Phycol.33:368–376, 1997.

587   Huang, C. J., Dong, Q.X., and Lin J.D.: Impact of global change on marine fisheries and
588   adaptation options. Journal of Oceanography in Taiwan Strait, 18(4): 481-494,
589   1999. (in Chinese with English abstract)

590   Hwang, J.H., Van, S. P., Choi, B.-J., Chang, Y. S., and Kim, Y. H.: The Physical
591   Processes in the Yellow Sea, Ocean & Coastal Management, 102 (2014), 449-
592   57, 2014.

593   Isobe, A.: Recent advances in ocean-circulation research on the Yellow Sea and East
594   China Sea shelves. J. Oceanagr. 64, 569e584, 2008.

595 Iversen, M.H., and Robert, M.L.: Ballasting effects of smectite on aggregate formation
596   and export from a natural plankton community. Mar. Chem. 175:18–27.
597   http://dx.doi.org/ 10.1016/j.marchem.2015.04.009, 2015.

598 Javier, R., Carlos, M.G., and Jaime, R.: Sedimentation loss of phytoplankton cells from
599   the mixed layer: effects of turbulence levels. Journal of Plankton Research.
600   18(9): 1727-1734. https://doi.org/10.1093/plankt/18.9.1727 , 1996.

601 Jokulsdottir, T., and Archer D.: A stochastic, Lagrangian model of sinking biogenic
602   aggregates in the ocean (SLAMS 1.0): model formulation, validation and
603   sensitivity. Geosci. Model Dev. 9. http://dx.doi.org/10.5194/gmd-9-1455-
604   2016, 2016.

605 Kodama T., Kurogi, H., Okazaki, M., Jinbo, T., and others.: Vertical distribution of
606   transparent exopolymer particle (TEP) concentration in the oligotrophic
607   western tropical North Pacific. Mar Ecol Prog Ser 513:29-37.
608   https://doi.org/10.3354/meps10954, 2014

609 Li, X., Feng, Y., Leng, X., Liu, H., and Sun, J.: Phytoplankton species composition of
610   four ecological provinces in Yellow Sea, China. Journal of Ocean University
611   of China, 16(6), 1115–1125. doi:10.1007/s11802-017-3270-3, 2017.

612 Lili, M. A., Chen, M., Guo, L., Lin, F., and Tong, J.: Distribution and source of
613   transparent exopolymer particles in the northern bering sea. Acta
614   Oceanologica Sinica, 34(5), 81-90, 2012.

615 Liu, H., Huang, Y., Zhai, W., Guo, S., Jin, H., and Sun, J.: Phytoplankton communities
616   and its controlling factors in summer and autumn in the southern Yellow Sea,
617   China. Acta Oceanologica Sinica, 34(2), 114–123. doi:10.1007/s13131-015-
618   0620-0, 2015a.

619 Liu, X., Huang, B., Huang, Q., Wang, L., Ni, X., Tang, Q., … Sun, J.: Seasonal
620   phytoplankton response to physical processes in the southern Yellow Sea.
621   Journal of Sea Research, 95, 45–55. doi: 10.1016/j.seares.2014.10.017, 2015b

622 Logan, B.E., Passow, U., Alldredge, A.L., Grossartt, H.P., and Simont, M.: Rapid
623   formation and sedimentation of large aggregates is predictable from
624   coagulation rates (halflives) of transparent exopolymer particles (TEP). Deep-
625   Sea Res. II 42 203–214, 1995.

626 Malpezzi, M.A，Sanford, L.P., and Crump, B.C.: Abundance and distribution of transparent exopolymer particles in the estuarine turbidity maximum of Chesapeake Bay.Marine Ecology Progress Series，486：23-35, 2013.

629 Mari, X.: Does ocean acidification induce an upward flux of marine aggregates[J]？ Biogeosciences，5（4）：1023-1031, 2008.

631 Mari, X., Rassoulzadegan, F., Brussaard, C.R.D., and Wassmann, P.: Dynamics of transparent exopolymeric particles (TEP) production by Phaeocystisglobosa under N- or Plimitation: a controlling factor of the retention/export balance. Harmful Algae 4: 895–914. http://dx.doi.org/10.1016/j.hal.2004.12.014, 2005.

635 Mari, X., Passow, U., Migon, C., Burd, A.B., and Legendre, L.: Transparent exopolymer particles: Effects on carbon cycling in the ocean. Progress in Oceanography, 151, 13–37. doi:10.1016/j.pocean.2016.11.002, 2017.

638 Mari, X., J.P. Torréton, C.B.T. Trinh, T. Bouvier, C.V. Thuoc, J.P. Lefebvre, and S.Ouillon.: Aggregation dynamics along a salinity gradient in the Bach Dang estuary, North Vietnam. Estuarine, Coastal and Shelf Science. 96: 151-158. https://doi.org/10.1016/j.ecss.2011.10.028, 2012.

642 Mopper, K., Zhou, J., Sri Ramana, K., Passow, U., Dam, H.G., and Drapeau, D.T.: The role of surface-active carbohydrates in the flocculation of a diatom bloom in a mesocosm. Deep-Sea Res. II Top. Stud. Oceanogr. 42:47–73. http://dx.doi.org/10.1016/0967- 0645(95)00004-A, 1995.

646 Mopper, K., Zhou, J., Sri Ramana, K., Passow, U., Dam, H.G., and Drapeau, D.T.: The role of surface-active carbohydrates in the flocculation of a diatom bloom in a mesocosm. Deep-Sea Res. II Top. Stud. Oceanogr. 42:47–73. http://dx.doi.org/10.1016/0967- 0645(95)00004-A, 1995.

650 Naimie, C.E., Blain, C.A., and Lynch, D.R.: Seasonal mean circulation in the Yellow Sea — a model-generated climatology. Continental Shelf Research 21(6-7), 667– 695. doi:10.1016/s0278-4343(00)00102-3, 2001.

653 Obernosterer. I., and Herndl, G.J.: Phytoplankton extracellular release and bacterial growth: dependence on inorganic N: P ratio. Marine Ecology Progress Series.116: 247-257. https://doi.org/10.3354/meps116247, 1995.

Orellana, M.V., Matrai, P.A., and Leck, C., Rauschenberg, C.D., Lee, A.M., and Coz, E.: Marine microgels as a source of cloud condensation nuclei in the high arctic. Proc. Natl. Acad. Sci. U. S. A. 108, 13612–13617, 2011.

Ortega-Retuerta, E., Duarte, C.M., and Reche, I.: Significance of Bacterial Activity for the Distribution and Dynamics of Transparent Exopolymer Particles in the Mediterranean Sea. Microbial Ecology, 59(4), 808–818. doi:10.1007/s00248-010-9640-7, 2010.

Ortega-Retuerta, E., Mazuecos, I.P., Reche, I., Gasol, J.M., Álvarez-Salgado, X.A., Álvarez, M., Montero, M.F., Arístegui, J.: Transparent Exopolymer Particle (TEP) distribution and in situ prokaryotic generation across the deep Mediterranean Sea and nearby North East Atlantic Ocean, Progress in Oceanography, doi: https://doi.org/10.1016/j.pocean.2019.03.002, 2019.

Ortega-Retuerta, E., Reche, I., Pulida-Villena, E., et al.: Uncoupled distributions of transparent exopolymer particles (TEP) and dissolved carbohydrates in the Southern Ocean.Marine Chemistry,115：59-65, 2009.

Parinos, C., Gogou, A., Krasakopoulou, E., Lagaria, A., Giannakourou, A., Karageorgis, A. P., & Psarra, S.: Transparent Exopolymer Particles (TEP) in the NE Aegean Sea frontal area: Seasonal dynamics under the influence of Black Sea water. Continental Shelf Research, 149, 112–123. doi:10.1016/j.csr.2017.03.012, 2017.

Passow, U.: Production of transparent exopolymer particles (TEP) by phyto- and bacterioplankton. Mar. Ecol. Prog. Ser. 236:1–12. http://dx.doi.org/10.3354/meps236001, 2002a.

Passow, U.: Transparent exopolymer particles (TEP) in aquatic environments. Prog. Oceanogr. 55 287–333, 2002b.

Passow, U., Alldredge, A.L., and Logan, B.E.: The role of particulate carbohydrate exudates in the flocculation of diatom blooms. Deep-Sea Res. I Oceanogr. Res. Pap. 41:335–357. http://dx.doi.org/10.1016/0967-0637(94)90007-8, 1994.

685   Passow, U., and Alldredge, A.L.: Distribution, size and bacterial-colonization of
686   transparent exopolymer particles (Tep) in theocean. Mar Ecol Prog Ser
687   113:185–198, 1994.

688   Passow, U., and Alldredge, A.L.: A dye-binding assay for the spectrophotometric
689   measurement of transparent exopolymer particles (TEP). Limnol. Oceanogr.
690   40, 1326–1335, 1995.

691   Passow, U., and Alldredge, A.L.: Do transparent exopolymer particles (TEP) inhibit
692   grazing by the euphausidEuphausiapacifica. J. Plankton Res. 21, 2203–2217,
693   1999.

694   Passow, U., Shipe, R.F., Murray, A., Pak, D.K., Brzezinski, M.A., and Alldredge, A.L.:
695   The origin of transparent exopolymerparticles (TEP) and their role in the
696   sedimentation of particulatematter. Cont Shelf Res 21:327–346, 2001.

697   Peng, A.G., and Huang, Y.P.: Study on TEP and its relationships with Uranium, Thorium,
698   Polonium Isotopes in Jiulong Estuary. Journal of Xiamen University.46(1):
699   38-42, 2007. (in Chinese with English abstract)

700   Prairie, J.C., Ziervogel, K., Camassa, R., McLaughlin, R.M., White, B.L., Dewald, C.,
701   and Arnosti, C.: Delayed settling of marine snow: effects of density gradient
702   and particle properties and implications for carbon cycling. Mar. Chem.
703   175:28–38. http://dx.doi.org/ 10.1016/j.marchem.2015.04.006, 2015.

704   Prieto, L., Navarro, G., Cózar, A., Echevarría, F., and García, C.M.: Distribution of TEP
705   in the euphotic and upper mesopelagic zones of the southern Iberian coasts.
706   Deep Sea Research II. 53(11-13): 1314-1328.
707   https://doi.org/10.1016/j.dsr2.2006.03.009, 2006.

708   Prieto, L., Ruiz, J., Echevarría, F., García, C.M., Bartual, A., Gálvez, J.A., Corzo, A., and
709   Macías, D.: Scales and processes in the aggregation of diatom blooms: high
710   time resolution and wide size range records in a mesocosm study. Deep Sea
711   Research II. 49: 1233-1253. https://doi.org/10.1016/S0967-0637(02)00024-9,
712   2002.

713   Radić, T., Kraus, R., Fuks, D., Radić, J., and Pečar, O.: Transparent exopolymeric
714   particles' distribution in the northern Adriatic and their relation to

microphytoplankton biomass and composition. Science of The Total Environment, 353(1-3), 151–161. doi: 10.1016/j.scitotenv.2005.09.013, 2005.

Ramaiah, N., Takeda, S., Furuya, K., Yoshimura, T., and others.: Effect of iron enrichment on the dynamics of transparent exopolymer particles in the western subarctic Pacific. Prog Oceanogr 64:253−261, 2005.

Ramaiah, N., Yoshikawa, T., and Furuya, K.: Temporal variations in transparent exopolymer particles (TEP) associated with a diatom spring bloom in a subarctic ria in Japan. Marine Ecology Progress Series. 212: 79-88. https://doi.org/10.3354/meps212079, 2001.

Rochelle-Newall, E.J., Mari, X., and Pringault, O.: Sticking properties of transparent exopolymeric particles (TEP) during aging and biodegradation. Journal of Plankton Research. 32(10): 1433-1442. https://doi.org/10.1093/plankt/fbq060

Ruiz, J., Macías, D., and Peters, F.: Turbulence increases the average settling velocity of phytoplankton cells. Proceeding of the National Academy of Science of the United States of America. 101(51): 17720-17724. https://doi.org/10.1073/pnas.0401539101, 2004.

Stoderegger, K., and Herndl, G.J.: Production of exopolymer particles by marine bacterioplankton under contrasting turbulence conditions. Marine Ecology Progress Series. 189: 9-16. https://doi.org/10.3354/meps189009, 1999.

Su, J.: Circulation dynamics of the China seas: north of 181N. In: Robinson, A.R., Brink, K., (Eds.), The Sea, vol. 11. The Global Coastal Ocean: Regional Studies and Syntheses. Wiley, New York,pp. 483–506, 1999, 1998.

Sun, C.C., Wang, Y.S., Wu, M.L., Li, N., Lin, L., Song, H., Wang, Y.T., Deng, C., Peng, Y.L., Sun, F.L., and Li, C.L.: Distribution of transparent exopolymer particles in the Pearl River Estuary in summer. Journal of Tropical Oceanography. 29(5): 81-87, 2010. (in Chinese with English abstract)

Surosz, W., Palinska, K. A., and Rutkowska, A.: Production of Transparent Exopolymer Particles (Tep) in the Nitrogen Fixing Cyanobacterium Anabaena Flos-*a*quae Ol-K10, Oceanologia, 48 (3). pp. 385–394, 2006.

744 Tang, Q. S., Jin, X.S., Wang, J., Zhuang, Z.M., Cui, Y., and Meng, T.X.: Decadal-scale
745   variations of ecosystem productivity and control mechanisms in the Bohai
746   Sea. Fisheries Oceanography, 12(4-5): 223-233, 2003.

747 Tang, Q.S., and Su, J. L.: Marine Ecosystem Dynamics Study of China. Key Scientific
748   Questions and Developing Strategies (in Chinese). Beijing: Science Press, 3–
749   34, 2001.

750 Tang, Q.S., Su, J.L., and Zhang, J.: China GLOBEC II: a case study of the Yellow Sea
751   and East China Sea ecosystem dynamics preface. Deep-Sea Res. II 57, 993–
752   995, 2010.

753 Tang, Q.S., Su, J.L., Kishi, M.J., and Oh, I.S.: An introduction to the Second China–
754   Japan– Korea Joint GLOBEC Symposium on the ecosystem structure, food
755   web trophodynamics and physical-biological processes in the Northwest
756   Pacific. J. Mar. Syst. 67, 203–204, 2007.

757 Ter-Braak, C.J.F., and Šmilauer, P.: CANOCO Reference Manual and CanoDraw for
758   Windows User's Guide: Software for Canonical Community Ordination
759   (Version 4.5). Microcomputer Power, Wageningen. Soil macrofauna in
760   organic and conventional coffee plantations in Brazil, 2002.

761 Thuy, N.T., Lin, J.C.-T., Juang, Y., and Huang, C.: Temporal variation and interaction of
762   full size spectrum Alcian blue stainable materials and water quality parameters
763   in a reservoir. Chemosphere 131:139–148.
764   http://dx.doi.org/10.1016/j.chemosphere.2015.03.023, 2015.

765 Tranvik, L.J., Sherr, E.B., and Sherr, B.F.: Uptake and utilization of colloidal DOM by
766   heterotrophic flagellates in seawater. Mar EcolProg Ser 92:301–309, 1993.

767 Turner, J.T.: Zooplankton fecal pellets, marine snow and sinking phytoplankton blooms.
768   Aquatic Microbial Ecology. 27: 57-102. https://doi.org/10.3354/ame027057,
769   1993, 2002.

770 Turner, J.T.: Zooplankton fecal pellets, marine snow, phytodetritus and the ocean's
771   biological pump. Progress in Oceanography. 130: 205-248.
772   https://doi.org/10.1016/j.pocean.2014.08.005, 2015.

773   Verdugo, P., Alldredge, A.L., Azam, F., Kirchman, D.L., Passow, U., and Santschi, P.H.:
774   The oceanic gel phase: a bridge in the DOM-POM continuum. Mar. Chem. 92,
775   67–85, 2004.

776   Vicente Villardón, J.L. MULTBIPLOT: A package for Multivariate Analysis using
777   Biplots. Departamento de Estadística. Universidad de Salamanca, 2015.
778   (http://biplot.usal.es/ClassicalBiplot/index.html)

779   Vicente, I.D., Ortega-Retuerta, E., Romera, O., Moreles-Baquero, R., and Reche, I.:
780   Contribution of transparent exopolymer particles to carbon sinking flux in an
781   oligotrophic reservoir. Biogeochemistry. 96: 13-23.
782   https://doi.org/10.1007/s10533-009-9342-8, 2009.

783   Welschmeyer, N. A.: Fluorometric analysis of chlorophyll-a in the presence of
784   chlorophyll-b and pheopigments [J]. Limnology and Oceanography，39 :
785   1985-1992, 1994 .

786   Wen, L., Sun, J., He, Q., Wang, D., and Wang, M.: Winter phytoplankton assemblages of
787   coastal Yellow Sea connected to Jiaozhou Bay, China. Journal of Ocean
788   University of China, 6(1), 40–46. doi:10.1007/s11802-006-0040-7, 2007.

789   Wetz, M. S., Robbins, M.C., and Paerl, H.W.: Transparent exopolymer particles (TEP)
790   in a river-dominated estuary: spatial and temporal distributions and an
791   assessment of controls upon TEP formation.Estuaries and Coasts，32（3）:
792   447-455, 2009.

793   Wurl, O., and Holmes, M.: The gelatinous nature of the sea-surface microlayer. Mar.
794   Chem. 110:89–97. http://dx.doi.org/10.1016/j.marchem.2008.02.009, 2008.

795   Wurl, O., Wurl, E., Miller, L., Johnson, K., and Vagle, S.: Formation and global
796   distribution of sea-surface microlayers. Biogeosciences 8:121–135.
797   http://dx.doi.org/10. 5194/bg-8-121-2011, 2011a.

798   Wurl, O., Miller, L., and Vagle, S.: Production and fate of transparent exopolymer
799   particles in the ocean. J. Geophys. Res. C: Oceans 116, 2011b.

800   Wurl, O., Miller, L., Röttgers, R., and Vagle, S.: The distribution and fate of surface-
801   active substances in the sea-surface microlayer and water column. Mar. Chem.
802   115:1–9. http://dx.doi.org/10.1016/j.marchem.2009.04.007, 2009.

803 Xu, S., Song, J., Li, X., Yuan, H., Li, N., Duan, L., and Sun, P.: Changes in nitrogen and
804   phosphorus and their effects on phytoplankton in the Bohai Sea. Chinese
805   Journal of Oceanology and Limnology 28(4), 945–952. doi:10.1007/s00343-
806   010-0005-3, 2010.

807 Yang, G., Wu, Z., Song, L., and Lu, X.: Seasonal Variation of Environmental Variables
808   and Phytoplankton Community Structure and Their Relationship in Liaodong
809   Bay of Bohai Sea, China. Journal of Ocean University of China, 17(4), 864–
810   878. doi:10.1007/s11802-018-3407-z, 2018.

811 Yuan, D., Zhu, J., Li, C., and Hu, D.: Cross-shelf circulation in the Yellow and East
812   China Seas indicated by MODIS satellite observations. J. Mar. Syst. 70
813   (2008), 134e149, 2008.

814 Zang, J., Tang, Y., Zou E., and Lie, H.-J.: Analysis of Yellow Sea circulation. Chinese
815   Science Bulletin, 48(S1), 12–20. doi:10.1007/bf02900935, 2003.

816 Zetsche, E.-M., and Ploug, H.: Marine chemistry special issue: Particles in aquatic
817   environments: From invisible exopolymers to sinking aggregates. Mar. Chem.
818   175, 1–4, 2015.

819 Zhang, F., Li, C.L., Sun, S., Wu, Y.L., and Ren, J.P.: Distribution patterns of chlorophyll
820   a in spring and autumn in association with hydrological features in the
821   southern Yellow Sea and northern East China Sea. Chin. J. Oceanol. Limnol.
822   27, 784–792, 2009.

823 Zhang, S., Leng, X., Feng, Y., Ding, C., Yang, Y., Wang, J., … Sun, J.: Ecological
824   provinces of spring phytoplankton in the Yellow Sea: species composition.
825   Acta Oceanologica Sinica, 35(8), 114–125. doi:10.1007/s13131-016-0872-3,
826   2016.

827

828

829

830

831

832

833

834

Table 1 Average statuses of temperature (^{o}C), salinity (PSU), nutrients (µmol/l), chl-a (µg/l), TEP (µg Xeq. L^{-1}) and TEP$_S$ (m d^{-1}) during study seasons.

Seasons	Seas	Temperature	Salinity	DIP	DIN	DSi	NH$_4$	NO$_3$	NO$_2$	Chl-a	TEP	TEP$_S$
Autumn (2014)	Bohai Sea	9.77	24.13	0.29	10.24	7.24	0.98	0.18	9.08	0.34	0.42	0.90
	North Yellow Sea	13.23	31.56	0.18	3.91	3.70	0.45	0.27	3.19	0.35	0.44	0.95
	South Yellow Sea	16.32	31.60	0.22	4.95	5.64	0.58	0.16	4.21	0.78	0.93	1.13
Summer (2015)	Bohai Sea	23.90	30.55	0.08	3.94	3.91	0.85	0.63	2.45	1.02	1.02	1.01
	North Yellow Sea	20.40	31.71	0.14	2.01	2.55	0.53	0.27	1.21	0.83	0.83	1.06
	South Yellow Sea	21.40	31.28	0.19	4.15	4.01	0.57	0.23	3.35	1.42	1.42	1.05
Winter (2015)	Bohai Sea	0.29	6.43	0.29	4.28	4.28	1.78	0.19	2.31	4.82	4.82	1.02
	North Yellow Sea	4.73	32.20	0.14	1.06	3.50	0.47	0.09	0.49	7.00	7.00	1.03

Table 2. Concentration of TEP ==in 0-50m depths at different== area from various reports.

Location		TEP (µg Xeq. L^{-1})	References
Seas	Ross Sea	1003	Hong et al. (1997)
	The Baltic Sea	145-322	Engel (2002)
	Adriatic Sea	4-14800	Radic et al. (2005)
	Arabian Sea	507-560	Prieto et al. (2006)
	Weddell Sea	0-48.9	Ortega-Retuerta et al. (2009)
	Mediterranean Sea	19.4-53.1	Ortega-Retuerta et al. (2010)
	Eastern Mediterranean Sea	116-420	Bar-Zeev et al. (2011)
	North Yellow Sea	0.19-23.20	This Study (2014-15)
	South Yellow Sea	0.19-11.99	This Study (2014-15)
Part of Oceans	Northeast Atlantic	20-60	Engel (2004)
	Northwest Atlantic	10-120	Engle (2004)
	Santa Barbara Low Strait	85-252	Passow and Alldredge (1995)
	Western subarctic North Pacific	40-190	Ramaiah et al. (2005)
	Eastern tropical North Pacific	22.5	Wurl et al. (2011b)
	Eastern subarctic North Pacific	28.7	Wurl et al. (2011b)
	Western tropical North Pacific	43.3	Kodama et al. (2014)
Estuaries	Pearl River Estuary	85-1235	Sun et al. (2010)
	Jiulong river estuary	530-720	Peng and Huang (2007)
	Changjiang Estuary	173.33-1423.33	Guo & Sun (2018)
	Newson Estuary	805-1801	Wetz et al. (2009)
Bays	Gulf of Aqaba	130-222	Bar-Zeev et al. (2009)
	Gulf of Cadiz	25-717	Garc et al. (2002)
	Chesapeake Bay	37-2820	Malpezzi et al. (2013)
	Bohai Sea	0.19-14.75	This Study (2014-15)

Table 3. Concentration of TEP in 50-100 depths at different area from various reports.

Location		TEP (μgXeq. L^{-1})	References
Bays	Bransfield Strait	0-346	Corzo et al. (2005)
	Gulf of Aqaba	106-228	Bar-Zeev e.t al. (2009)
	Bohai Sea	0.39-4.33	This Study (2014-15)
Part of Oceans	Eastern tropical North Pacific	9.2	Wurl et al. (2011b)
	Eastern subarctic North Pacific	11.6	Wurl et al. (2011b)
	Western tropical North Pacific	42.2	Kodama et al. (2014
Seas	Mediterranean Sea	9.1-94.3	Ortega-Retuerta et al. (2010)
	Eastern Mediterranean Sea	48-189	Bar-Zeev et al. (2011)
	North Yellow Sea	0.19-11.01	This Study (2014-15)
	South Yellow Sea	0.2-0.79	This Study (2014-15)

Table 5. Seasonal average TEP distribution in surface area from various research with their minimum to maximum ranges.

Seasons	Location	TEP (µg Xeq. L^{-1})	References
Autumn	Aegean Sea	42.1	Parinos et al. 2017
	Bohai Sea	0.42	This Study (2014-15)
	North Yellow Sea	0.44	This Study (2014-15)
	South Yellow Sea	0.93	This Study (2014-15)
Spring	Changjiang Estuary	506.67	Guo & Sun (20180
	Aegean Sea	93.3	Parinos et al. 2017
	Northeast coast of Japan	1021.50	Ramaiah et al. (2001)
	Southern Iberian coasts	533.50	Prieto et al. (2006)
Summer	Changjiang Estuary	948.33	Guo & Sun (2018)
	Baltic Sea	233.50	Engel (2002)
	Aegean Sea	81.1	Parinos et al. 2017
	Northeast Atlantic Ocean	65.00	Engel (2004)
	Bransfield Strait	173.00	Corzo et al. (2005)
	Jiulong estuary	625.00	Peng and Huang (2007)
	Pearl River estuary	660.00	Sun et al. (2010)
	Bohai Sea	1.02	This Study (2014-15)
	North Yellow Sea	0.83	This Study (2014-15)
	South Yellow Sea	1.42	This Study (2014-15)
Winter	Bohai Sea	4.82	This Study (2014-15)
	North Yellow Sea	7.00	This Study (2014-15)

Table 5. Seasonal average sedimentation rates of TEP in different locations with their maximum and minimum ranges from different reports.

Seasons	Location	TEPs (mD^{-1})	References
Autumn	Bohai Sea	0.90	This Study (2014-15)
	North Yellow Sea	0.95	This Study (2014-15)
	South Yellow Sea	1.13	This Study (2014-15)
Spring	Changjiang Estuary	0.33	Guo & Sun (2018)
	Santa Barbara Strait	-0.22 ~0.04	Azetsu-Scott and Passow (2004)
Summer	Changjiang Estuary	0.59	Guo & Sun (2018)
	Bohai Sea	1.01	This Study (2014-15)
	North Yellow Sea	1.06	This Study (2014-15)
	South Yellow Sea	1.05	This Study (2014-15)
Winter	South Pacific Ocean	-0.29 ~0.49	Mari (20080
	Bohai Sea	1.02	This Study (2014-15)
	North Yellow Sea	1.03	This Study (2014-15)
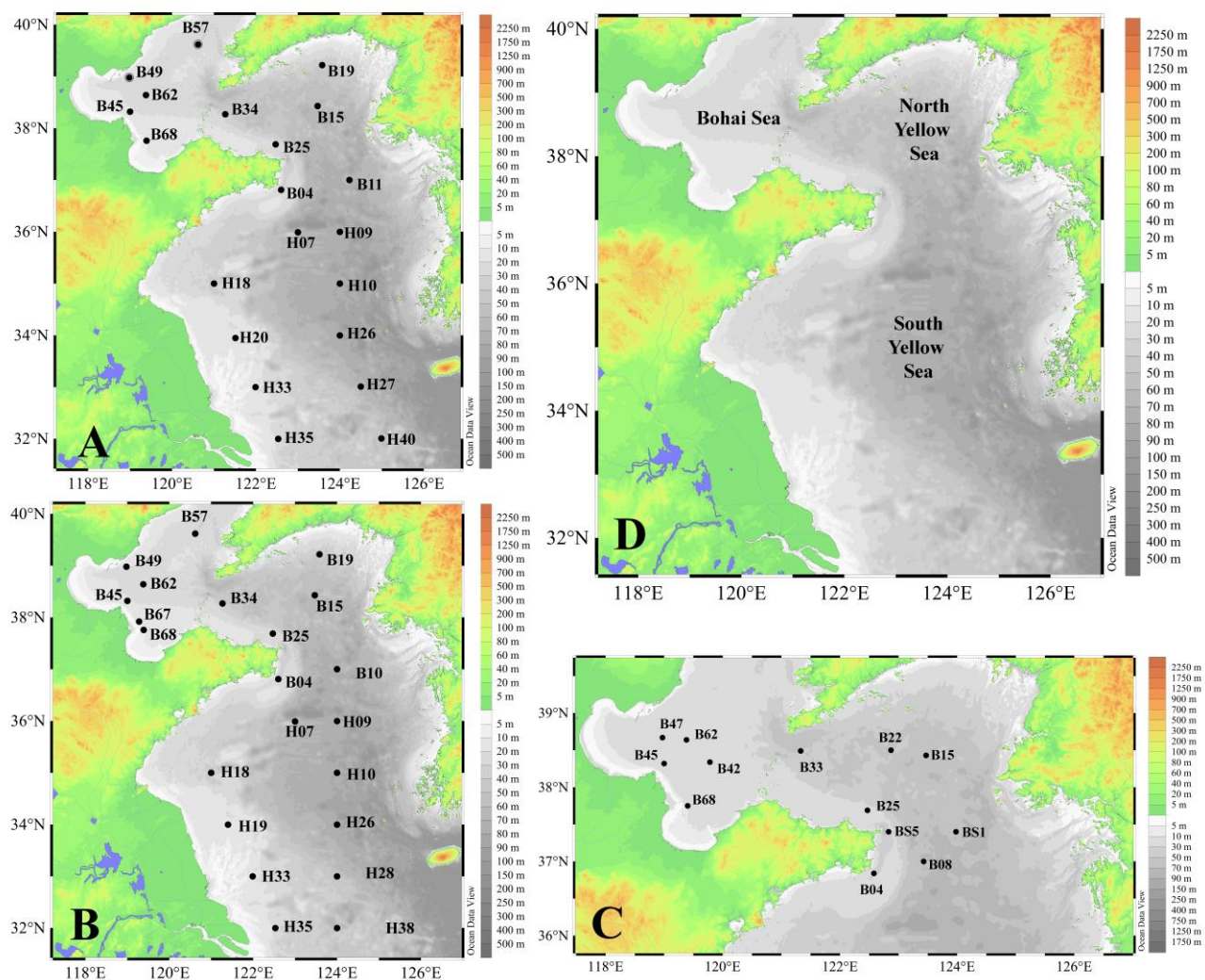
Figure 1. Study stations in map of autumn 2014 (A), summer 2015 (B) and winter 2015 (C) with their oceanic segmentation (D).
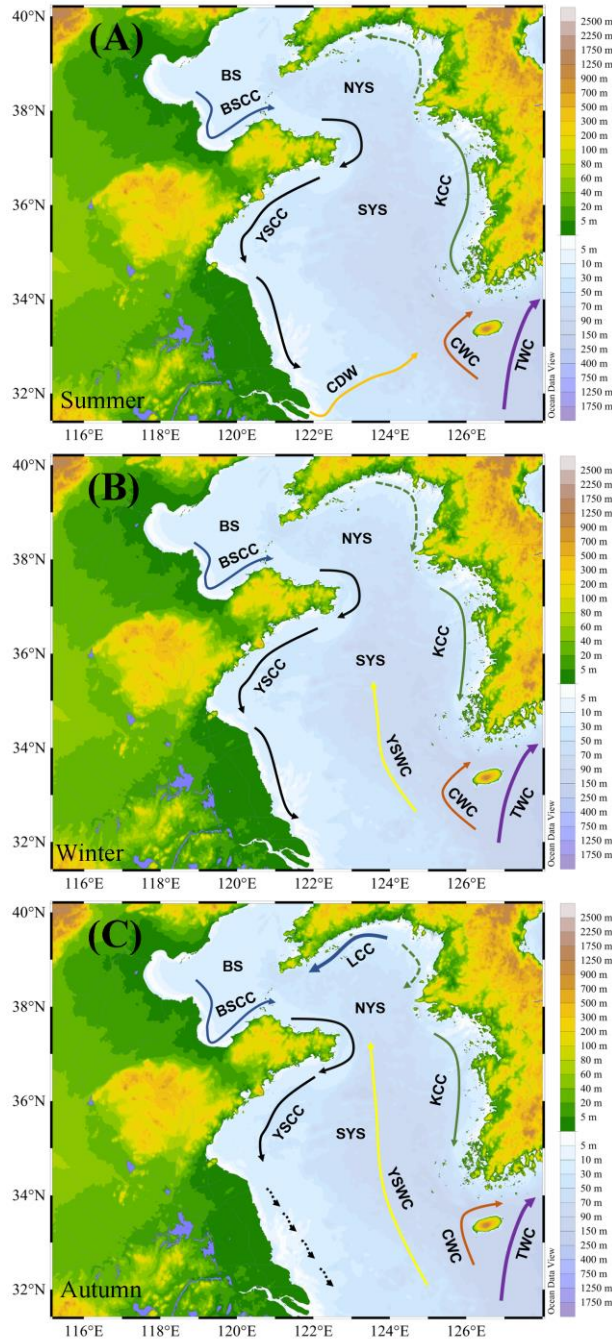
Figure 2. Direction of Currents at Bohai Sea (BS=Bohai Sea, BSCC=Bohai Sea coastal current), North Yellow Sea (NYS=North Yellow Sea, KCC=Korean Costal Current, LCC=Liaonan coastal current, YSCC=Yellow Sea Costal Current) and South Yellow Sea (SYS=South Yellow Sea, YSWC=Yellow Sea Warm Sea, CDW=Changiang Diluted Water, CWC= Cheju Warm Current, TWC=Tsushima Warm Current) during summer (a), winter (b) and autumn (c) seasons (Collaboratively modified after Hwang et al. 2014; Su 1998; Yuan et al. 2008; Isobe 2008, Zhang et al. 2003).
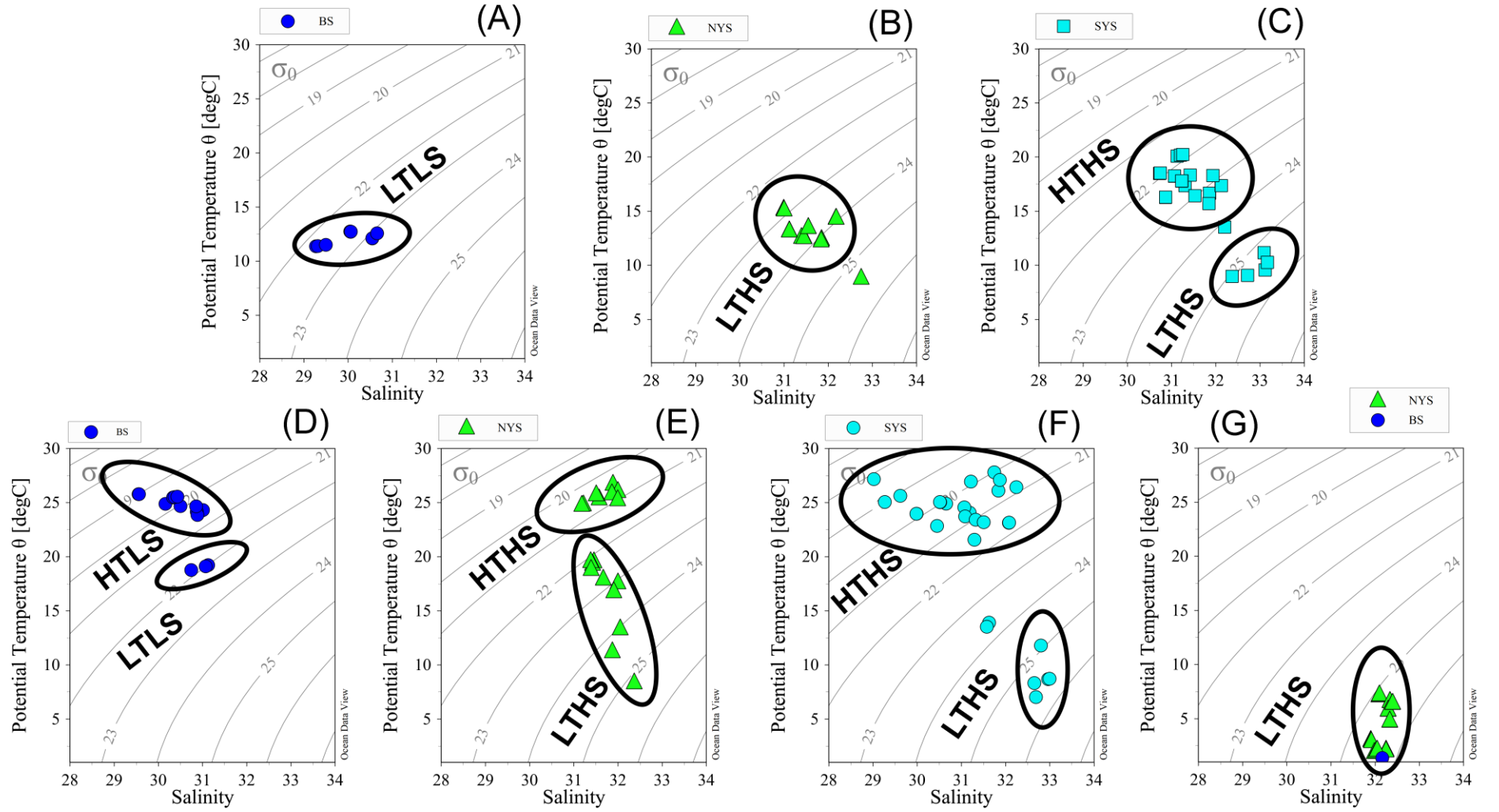
Figure 3. Density based seasonal water masses during autumn (A, B, C), summer (D, E, F) and winter (G) of BS (A, D, G), NYS (B, E, G) and SYS (C, F).
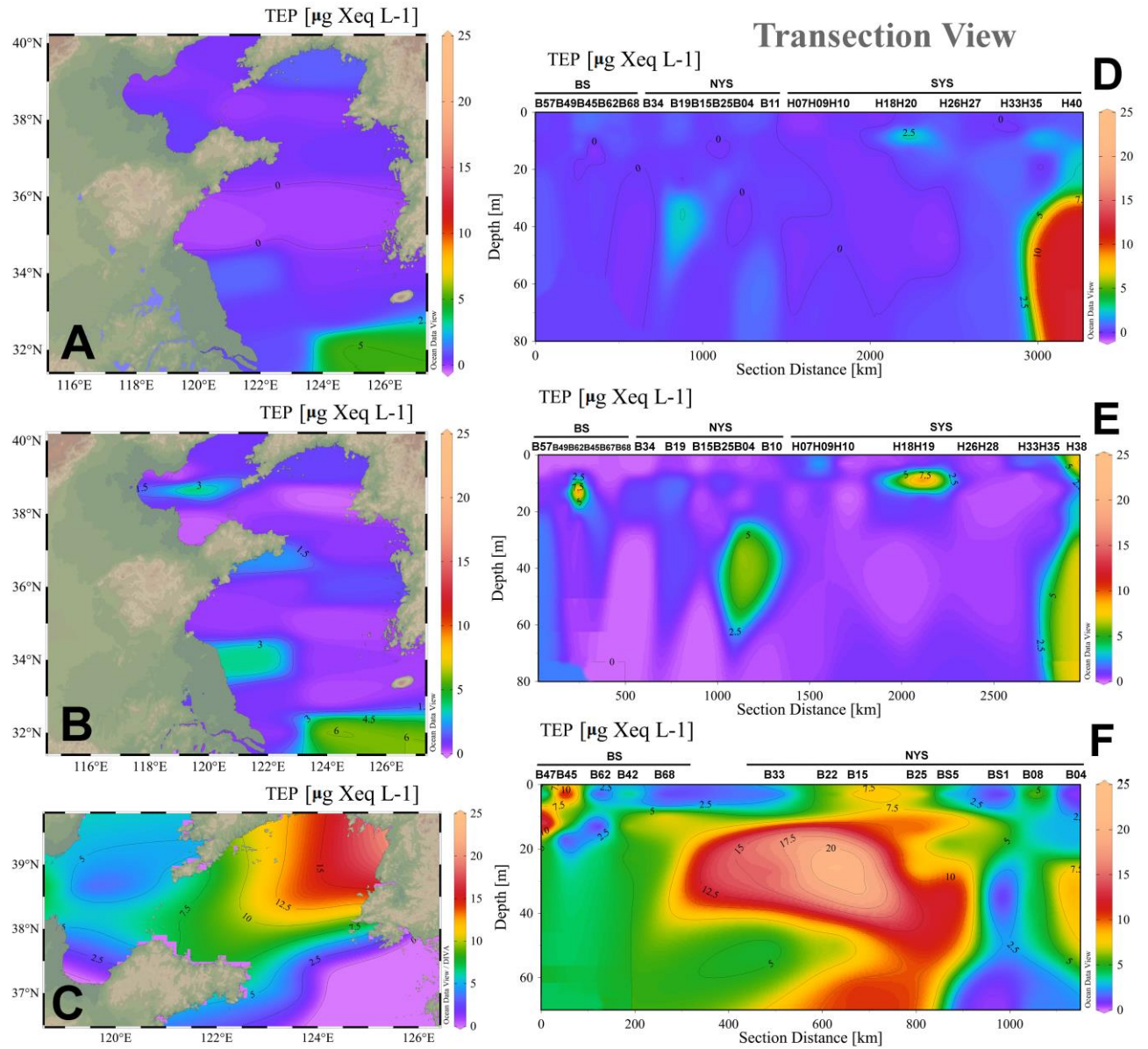
Figure 4. Average seasonal concentrations of TEP (A, B & C) with sectional view (D, E & F) of BS (D), NYS (E) and SYS (F) during autumn (A), summer (B) and winter (C).
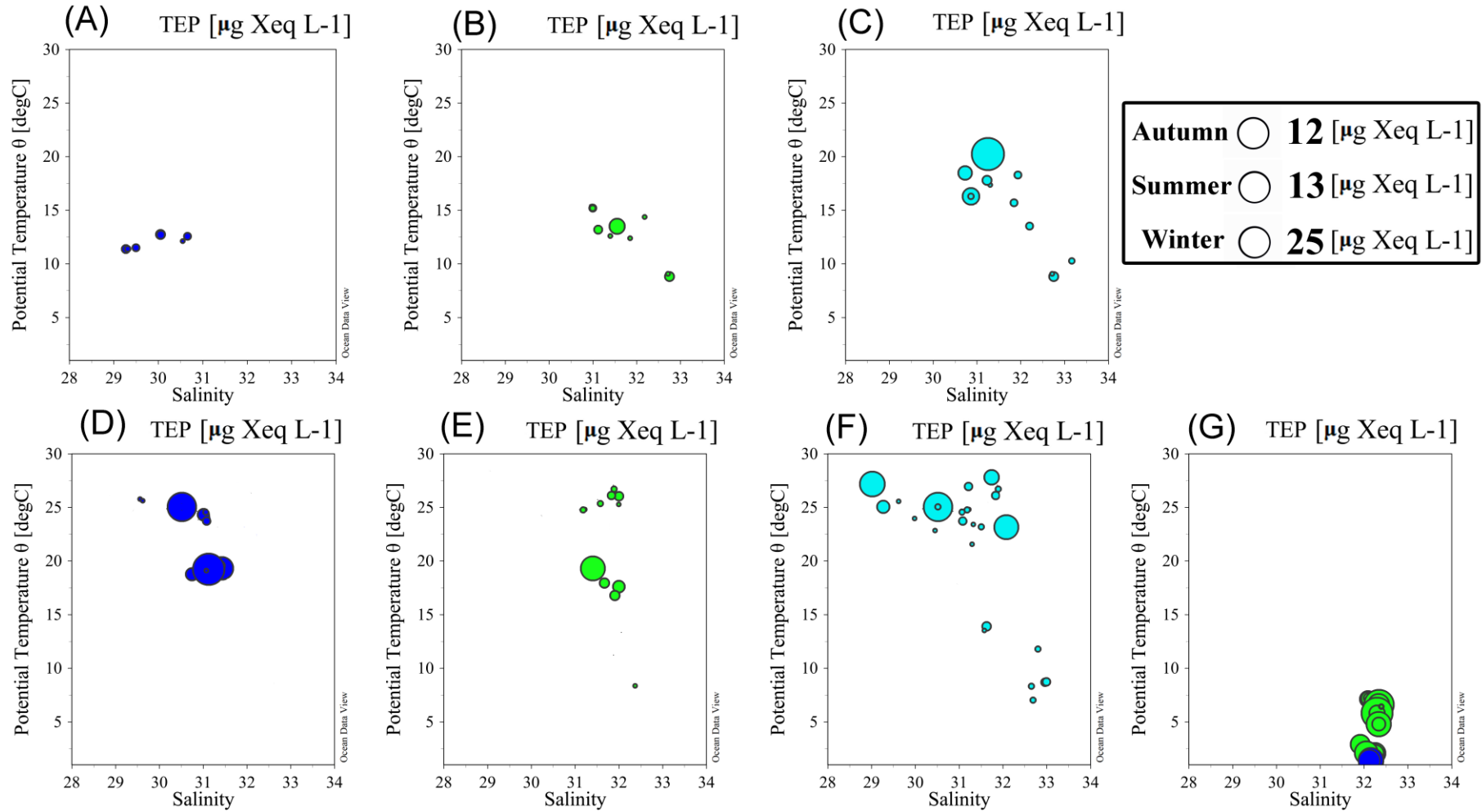
Figure 5. Seasonal TEP aggregations at different water mass during autumn (A, B, C), summer (D, E, F) and winter (G) of BS (A, D, G), NYS (B, E, G) and SYS (C, F).
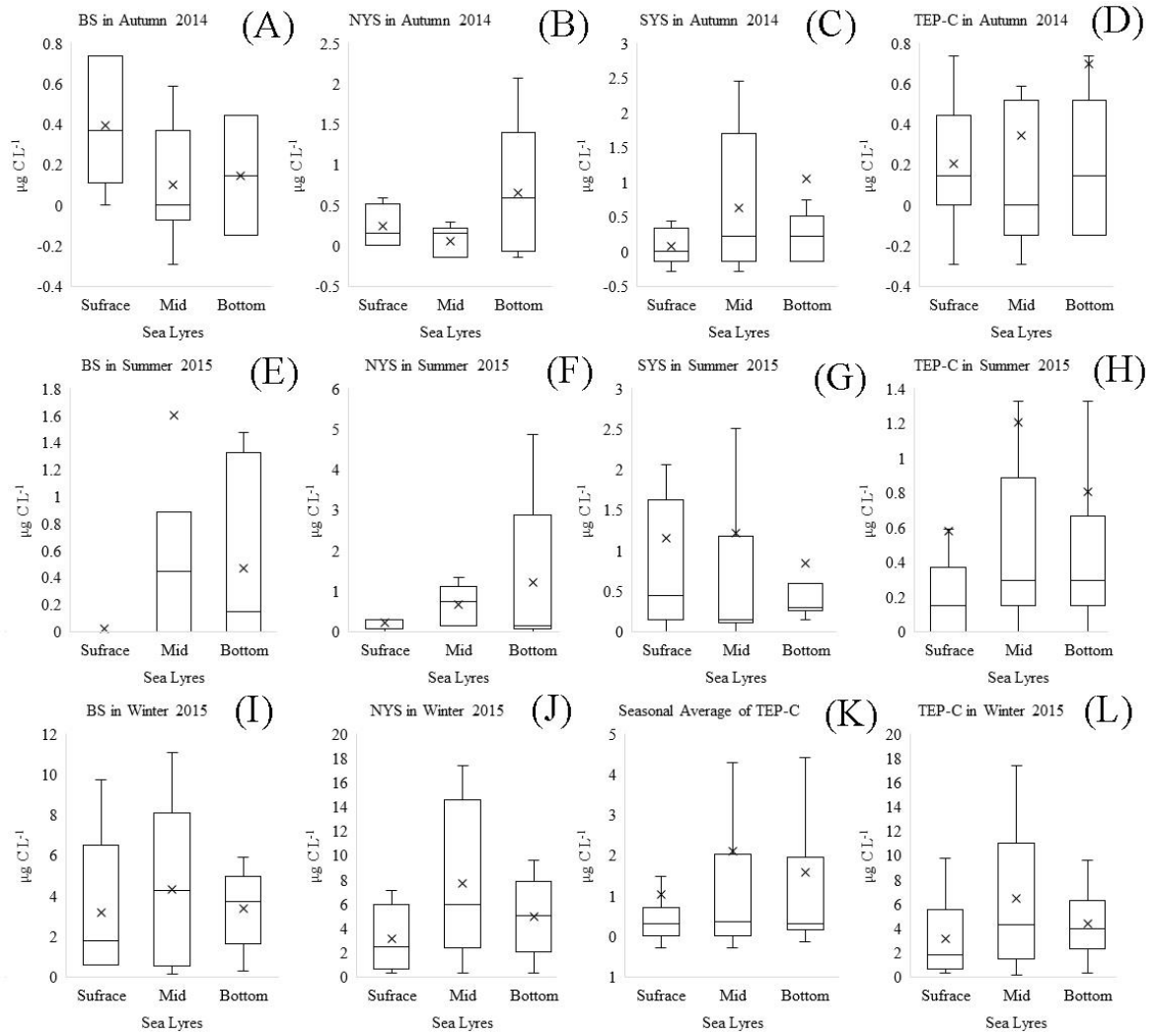
Figure 6. TEP associated carbon concentration during all seasons in Bohai Sea (A=autumn 2014, E=summer 2015, I=winter 2015), North Yellow Sea (B=autumn 2014, F=summer 2015, J=winter 2015), South Yellow Sea (C=Autumn 2014, G=summer 2015) with all data in average (K), autumn 2014 (D), summer 2015 (H) and winter 2015(L).
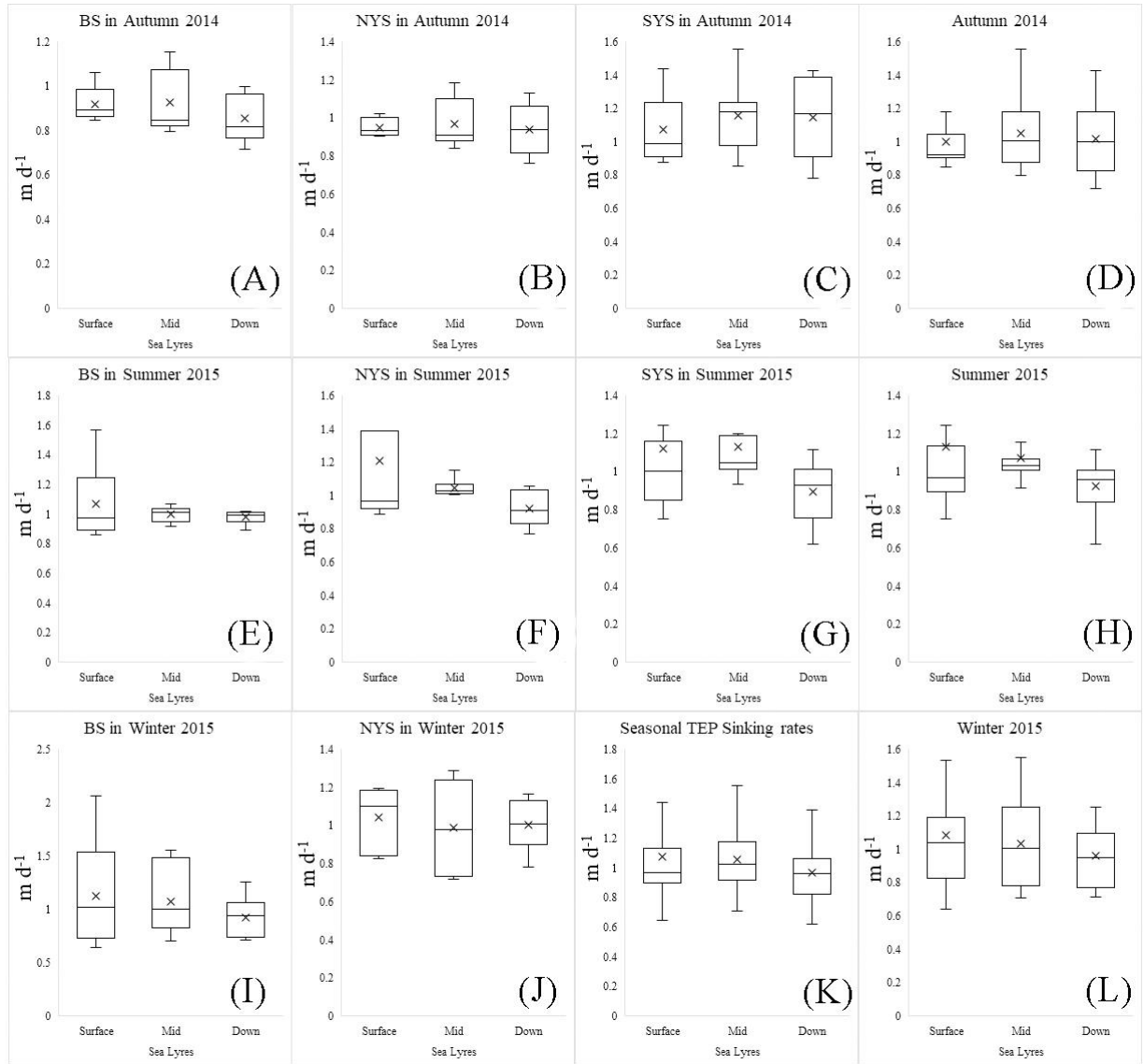
Figure 7. TEP sinking flux during all seasons in Bohai Sea (A=autumn 2014, E=summer 2015, I=winter 2015), North Yellow Sea (B=autumn 2014, F=summer 2015, J=winter 2015), South Yellow Sea (C=autumn 2014, G=summer 2015) with all seasonal sinking data in average (K), autumn 2014 (D), summer 2015 (H) and winter 2015(L).

Figure 8. CCA analysis among biotic and abiotic parameters of all study areas. Seasonal average i.e. autumn 2014 (A), summer 2015 (B), winter 2015(C) and total (L) with the CCA of all parameters according to locations i.e. Bohai Sea (D=autumn 2014, E=summer 2015,

F=winter 2015), North Yellow Sea (G=Autumn 2014, H=summer 2015, I=winter 2015) and South Yellow Sea (J=autumn 2014, K=summer 2015).
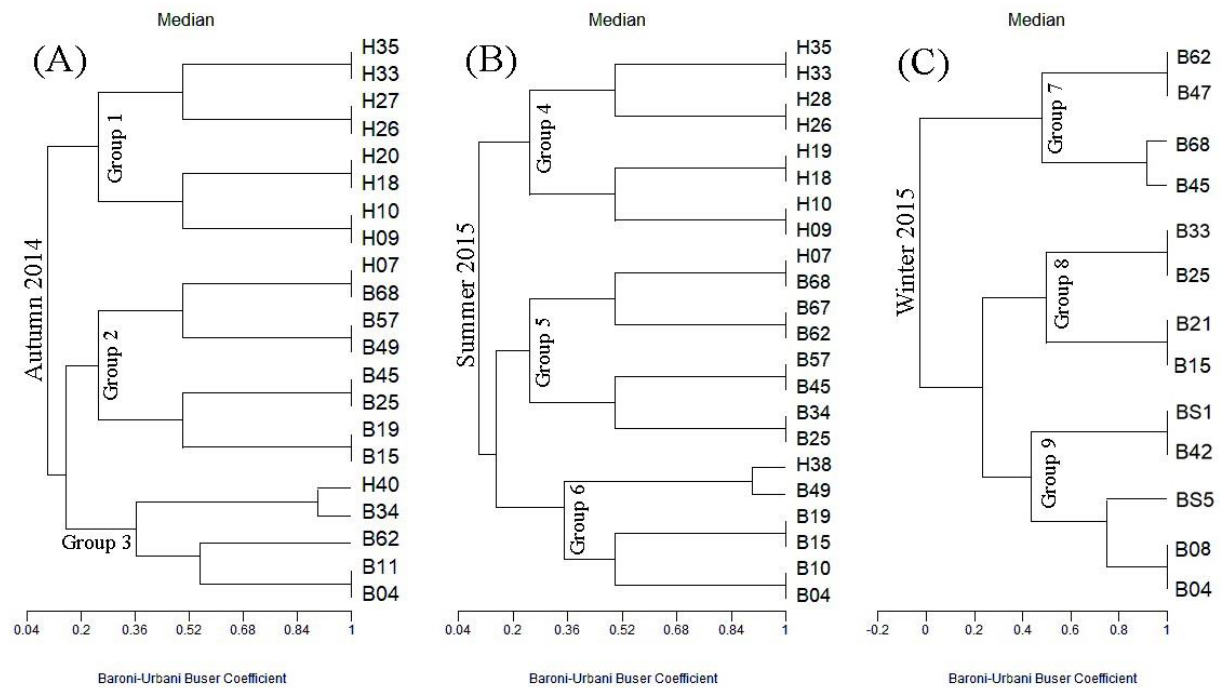

Figure 9. Seasonal Cluster analysis among related study stations of study area by considering all parameters and TEP, segmented by seasons i.e. autumn 2014 (A), summer 2015 (B) and

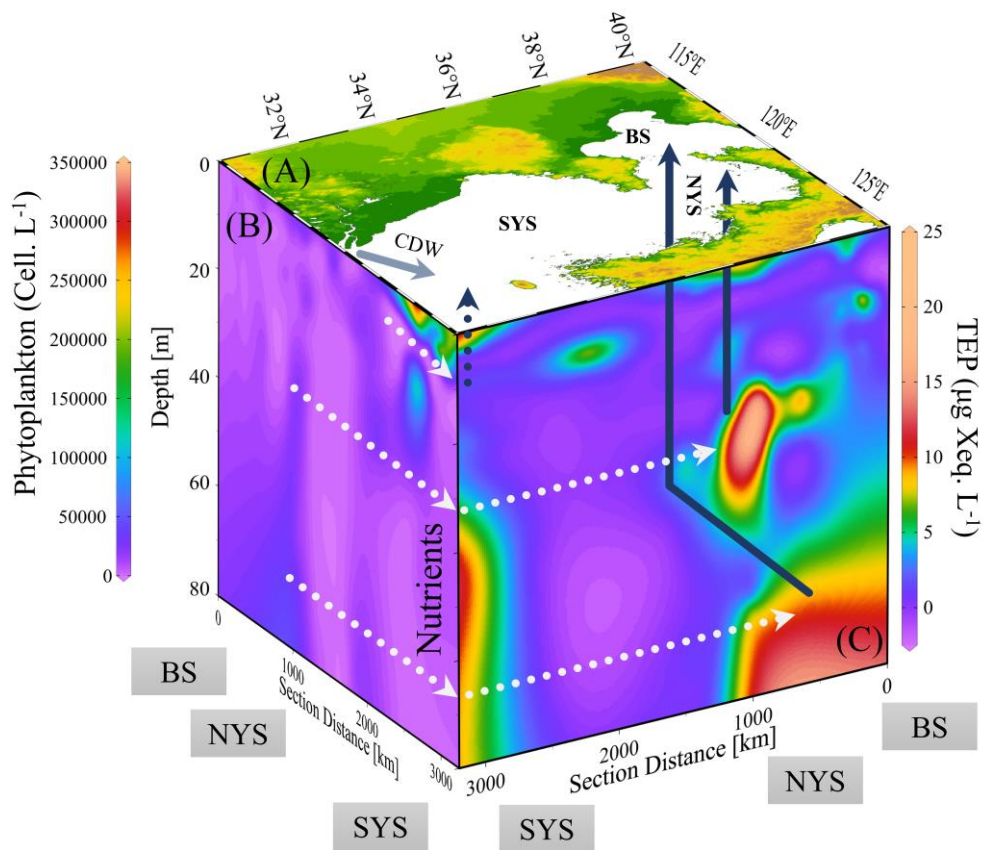winter 2015 (C). Groups (1-9) are indicating clustered group of closely related stations.

Figure 10. Conceptual model of seasonal average TEP aggregations (C) along study area (A) under the influences of phytoplankton (B). Arrows are projecting the relations (White arrows) and influences of assemblage (Blue arrows) through particular distances of associated seas.